

*Series capacitor installation
at Goshen Substation,
Goshen, Idaho, USA rated
at 395 kV, 965 Mvar
(Courtesy of PacifiCorp)*



5

TRANSMISSION LINES: STEADY-STATE OPERATION

In this chapter, we analyze the performance of single-phase and balanced three-phase transmission lines under normal steady-state operating conditions. Expressions for voltage and current at any point along a line are developed, where the distributed nature of the series impedance and shunt admittance is taken into account. A line is treated here as a two-port network for which the $ABCD$ parameters and an equivalent π circuit are derived. Also, approximations are given for a medium-length line lumping the shunt admittance, for a short line neglecting the shunt admittance, and for a lossless line assuming zero series resistance and shunt conductance. The concepts of *surge impedance loading* and transmission-line *wavelength* are also presented.

An important issue discussed in this chapter is *voltage regulation*. Transmission-line voltages are generally high during light load periods and

low during heavy load periods. Voltage regulation, defined in Section 5.1, refers to the change in line voltage as line loading varies from no-load to full load.

Another important issue discussed here is line loadability. Three major line-loading limits are: (1) the thermal limit, (2) the voltage-drop limit, and (3) the steady-state stability limit. Thermal and voltage-drop limits are discussed in Section 5.1. The theoretical steady-state stability limit, discussed in Section 5.4 for lossless lines and in Section 5.5 for lossy lines, refers to the ability of synchronous machines at the ends of a line to remain in synchronism. Practical line loadability is discussed in Section 5.6.

In Section 5.7 we discuss line compensation techniques for improving voltage regulation and for raising line loadings closer to the thermal limit.

CASE STUDY

High Voltage Direct Current (HVDC) applications embedded within ac power system grids have many benefits. A bipolar HVDC transmission line has only two insulated sets of conductors versus three for an ac transmission line. As such, HVDC transmission lines have smaller transmission towers, narrower rights-of-way, and lower line losses compared to ac lines with similar capacity. The resulting cost savings can offset the higher converter station costs of HVDC. Further, HVDC may be the only feasible method to: (1) interconnect two asynchronous ac networks; (2) utilize long underground or underwater cable circuits; (3) bypass network congestion; (4) reduce fault currents; (5) share utility rights-of-way without degrading reliability; and (6) mitigate environmental concerns. The following article provides an overview of HVDC along with HVDC applications [6].

The ABCs of HVDC Transmission Technologies: An Overview of High Voltage Direct Current Systems and Applications

BY MICHAEL P. BAHRMAN
AND BRIAN K. JOHNSON

High voltage direct current (HVDC) technology has characteristics that make it especially attractive for certain transmission applications. HVDC transmission is widely recognized as being advantageous for long-distance bulk-power delivery, asynchronous interconnections, and long submarine cable crossings. The number of HVDC projects committed or under consideration globally has increased in recent years reflecting a renewed interest in this mature technology. New converter designs have broadened

the potential range of HVDC transmission to include applications for underground, offshore, economic replacement of reliability-must-run generation, and voltage stabilization. This broader range of applications has contributed to the recent growth of HVDC transmission. There are approximately ten new HVDC projects under construction or active consideration in North America along with many more projects underway globally. Figure 1 shows the Danish terminal for Skagerrak's pole 3, which is rated 440 MW. Figure 2 shows the ± 500 -kV HVDC transmission line for the 2,000 MW Intermountain Power Project between Utah and California. This article discusses HVDC technologies, application areas where HVDC is favorable compared to ac transmission, system configuration, station design, and operating principles.

("The ABCs of HVDC Transmission Technologies" by Michael P. Bahrman and Brian K. Johnson. © 2007 IEEE. Reprinted, with permission, from IEEE Power & Energy Magazine, March/April 2007)

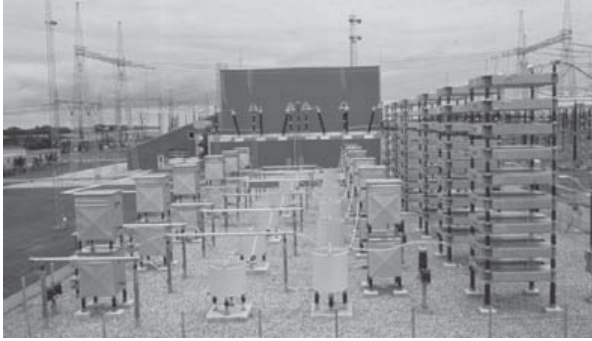


Figure 1
HVDC converter station with ac filters in the foreground and valve hall in the background



Figure 2
A ± 500 -kV HVDC transmission line

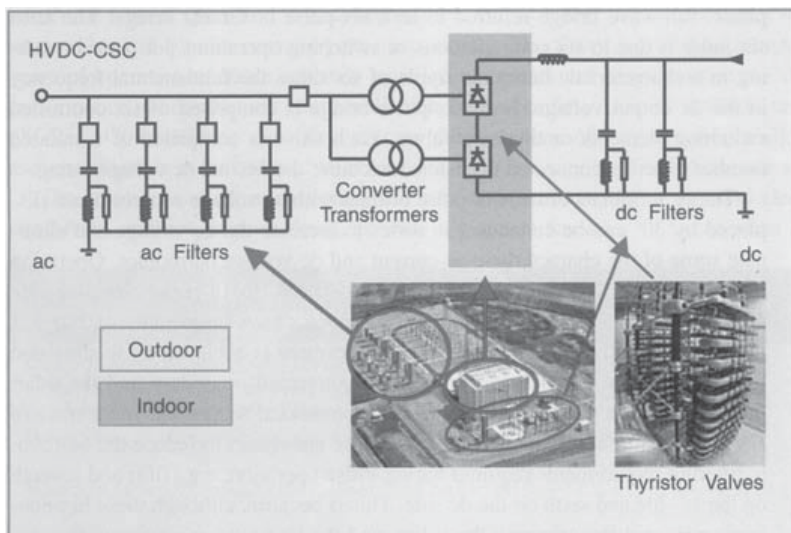


Figure 3
Conventional HVDC with current source converters

CORE HVDC TECHNOLOGIES

Two basic converter technologies are used in modern HVDC transmission systems. These are conventional line-commutated current source converters (CSCs) and self-commutated voltage source converters (VSCs). Figure 3 shows a conventional HVDC converter station with CSCs while Figure 4 shows a HVDC converter station with VSCs.

LINE-COMMUTATED CURRENT SOURCE CONVERTER

Conventional HVDC transmission employs line-commutated CSCs with thyristor valves. Such converters require a synchronous voltage source in order to operate. The basic building block used for HVDC conversion is the three-phase, full-wave bridge referred to as a six-pulse or Graetz bridge. The term six-pulse is due to six commutations or switching operations per period resulting in a characteristic harmonic ripple of six times the fundamental frequency in the dc output voltage. Each six-pulse bridge is comprised of six controlled switching elements or thyristor valves. Each valve is comprised of a suitable number of series-connected thyristors to achieve the desired dc voltage rating.

The dc terminals of two six-pulse bridges with ac voltage sources phase displaced by 30° can be connected in series to increase the dc voltage and eliminate some of the characteristic ac current and dc voltage harmonics. Operation in this manner is referred to as 12-pulse operation. In 12-pulse operation, the characteristic ac current and dc voltage harmonics have frequencies of $12n \pm 1$ and $12n$, respectively. The 30° phase displacement is achieved by feeding one bridge through a transformer with a wye-connected secondary and the other bridge through a transformer with a delta-connected secondary. Most modern HVDC transmission schemes utilize 12-pulse converters to reduce the harmonic filtering requirements required for six-pulse operation; e.g., fifth and seventh on the ac side and sixth on the dc side. This is because, although these harmonic currents still flow through the valves and the transformer windings, they are 180° out of phase and cancel out on the primary side of the converter transformer. Figure 5 shows the thyristor valve arrangement for a 12-pulse converter with three quadruple valves, one for each phase. Each thyristor valve is built up with series-connected thyristor modules.

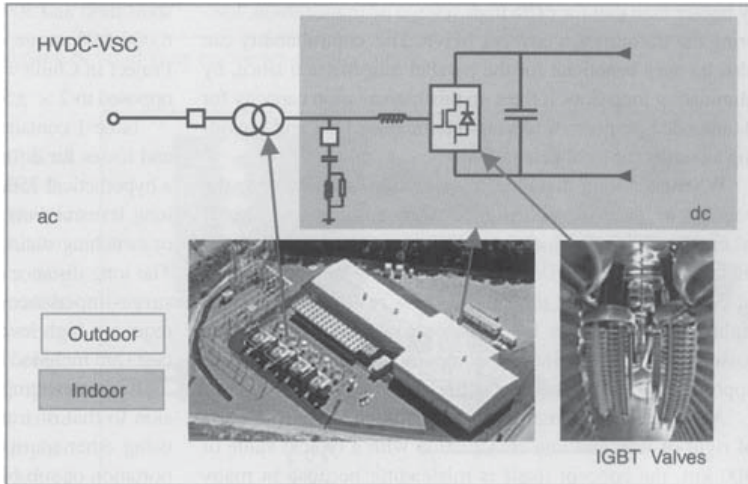


Figure 4
HVDC with voltage source converters

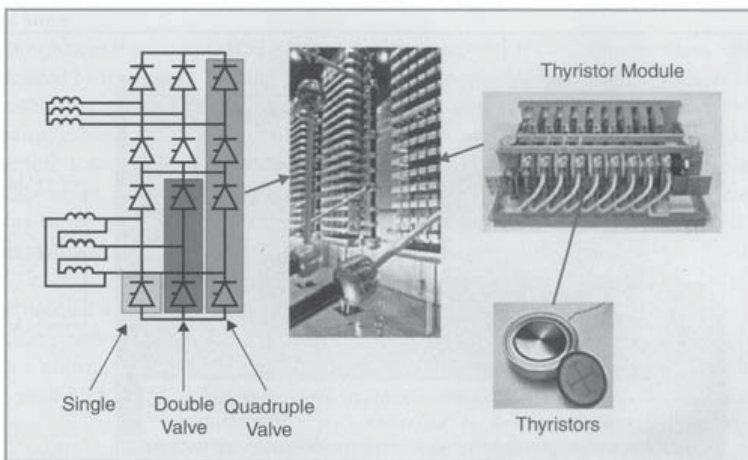


Figure 5
Thyristor valve arrangement for a 12-pulse converter with three quadruple valves, one for each phase

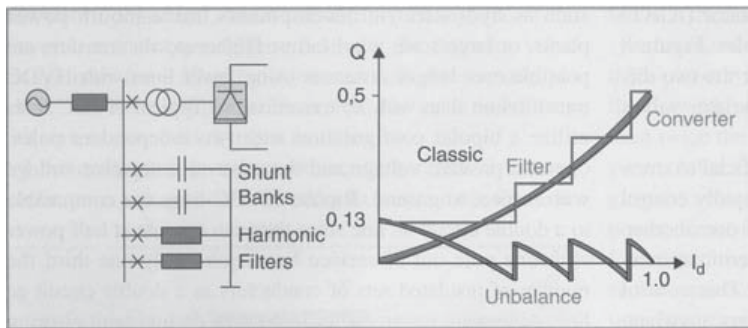


Figure 6
Reactive power compensation for conventional HVDC converter station

Line-commutated converters require a relatively strong synchronous voltage source in order to commute. Commutation is the transfer of current from one phase to another in a synchronized firing sequence of the thyristor valves. The three-phase symmetrical short circuit capacity available from the network at the converter connection point should be at least twice the converter rating for converter operation. Line-commutated CSCs can only operate with the ac current lagging the voltage, so the conversion process demands reactive power. Reactive power is supplied from the ac filters, which look capacitive at the fundamental frequency, shunt banks, or series capacitors that are an integral part of the converter station. Any surplus or deficit in reactive power from these local sources must be accommodated by the ac system. This difference in reactive power needs to be kept within a given band to keep the ac voltage within the desired tolerance. The weaker the ac system or the further the converter is away from generation, the tighter the reactive power exchange must be to stay within the desired voltage tolerance. Figure 6 illustrates the reactive power demand, reactive power compensation, and reactive power exchange with the ac network as a function of dc load current.

Converters with series capacitors connected between the valves and the transformers were introduced in the late 1990s for weak-system, back-to-back applications. These converters are referred to as capacitor-commutated converters (CCCs). The series capacitor provides some of the converter reactive power compensation requirements automatically with load current and provides part of the commutation voltage, improving voltage stability. The overvoltage protection of the series capacitors is simple since the capacitor is not exposed to line faults, and the fault current for internal converter faults is limited by the impedance of the converter transformers. The CCC configuration allows higher power ratings in areas where the ac network is close to its voltage stability limit. The asynchronous Garabi interconnection between Brazil and Argentina consists of 4×550 MW parallel CCC links. The Rapid City Tie between the Eastern and Western interconnected systems consists of 2×10 MW parallel CCC links (Figure 7). Both installations use a modular design with

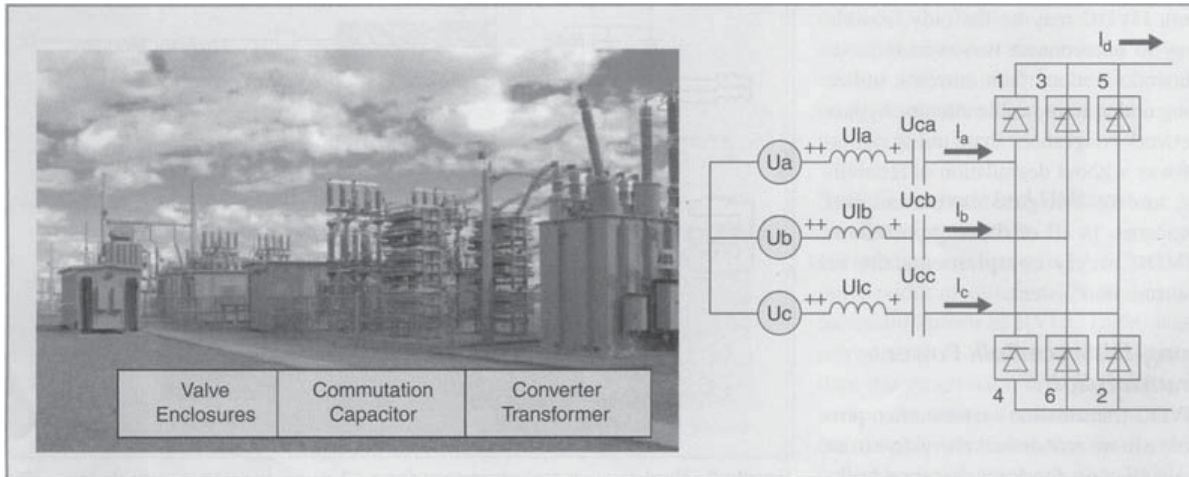


Figure 7

Asynchronous back-to-back tie with capacitor-commutated converter near Rapid City, South Dakota

converter valves located within prefabricated electrical enclosures rather than a conventional valve hall.

SELF-COMMUTATED VOLTAGE SOURCE CONVERTER

HVDC transmission using VSCs with pulse-width modulation (PWM), commercially known as HVDC Light, was introduced in the late 1990s. Since then the progression to higher voltage and power ratings for these

converters has roughly paralleled that for thyristor valve converters in the 1970s. These VSC-based systems are self-commutated with insulated-gate bipolar transistor (IGBT) valves and solid-dielectric extruded HVDC cables. Figure 8 illustrates solid-state converter development for the two different types of converter technologies using thyristor valves and IGBT valves.

HVDC transmission with VSCs can be beneficial to overall system performance. VSC technology can rapidly control both active and reactive power independently of one another. Reactive power can also be controlled at each terminal independent of the dc transmission voltage level. This control capability gives total flexibility to place converters anywhere in the ac network since there is no restriction on minimum network short-circuit capacity. Self-commutation with VSC even permits black start; i.e., the converter can be used to synthesize a balanced set of three phase voltages like a virtual synchronous generator. The dynamic support of the ac voltage at each converter terminal improves the voltage stability and can increase the transfer capability of the sending- and receiving-end ac systems, thereby leveraging the transfer capability of the dc link. Figure 9 shows the IGBT converter valve arrangement for a VSC station. Figure 10 shows the active and reactive power operating range for a converter station with a VSC. Unlike conventional HVDC transmission, the converters themselves have

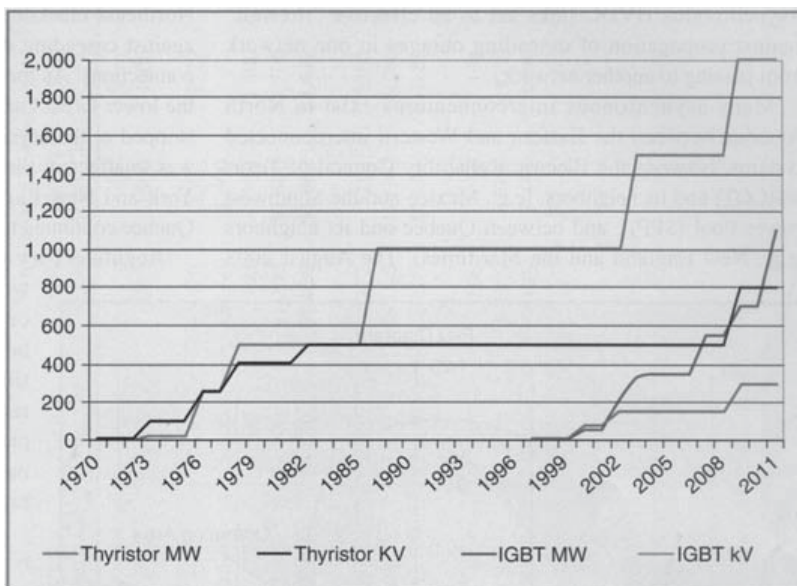


Figure 8

Solid-state converter development

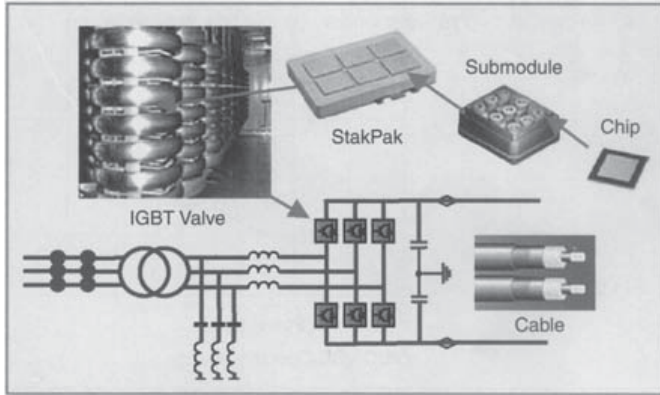


Figure 9
HVDC IGBT valve converter arrangement

no reactive power demand and can actually control their reactive power to regulate ac system voltage just like a generator.

HVDC APPLICATIONS

HVDC transmission applications can be broken down into different basic categories. Although the rationale for

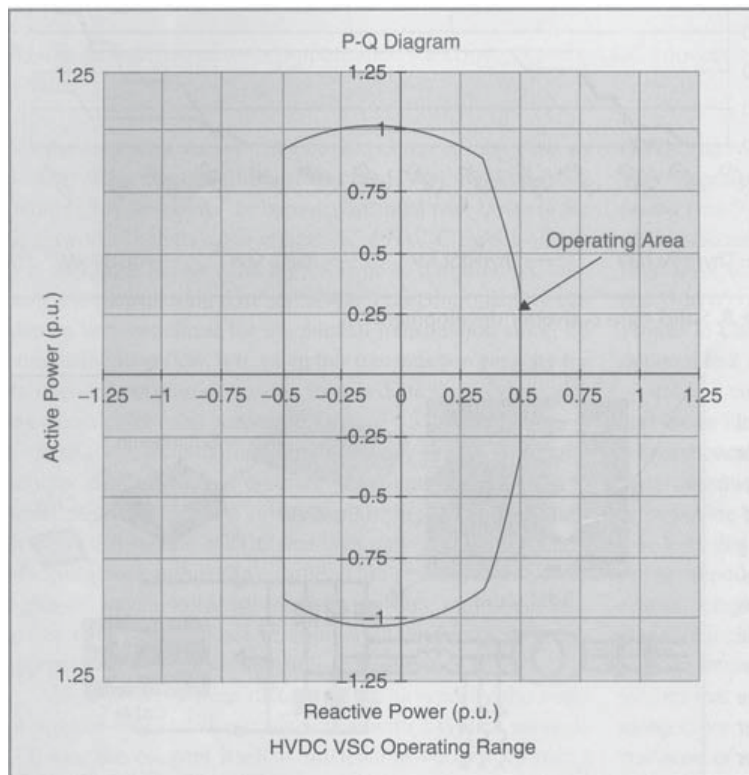


Figure 10
Operating range for voltage source converter HVDC transmission

selection of HVDC is often economic, there may be other reasons for its selection. HVDC may be the only feasible way to interconnect two asynchronous networks, reduce fault currents, utilize long underground cable circuits, bypass network congestion, share utility rights-of-way without degradation of reliability, and to mitigate environmental concerns. In all of these applications, HVDC nicely complements the ac transmission system.

LONG-DISTANCE BULK POWER TRANSMISSION

HVDC transmission systems often provide a more economical alternative to ac transmission for long-distance bulk-power delivery from remote resources such as hydroelectric developments, mine-mouth power plants, or large-scale wind farms. Higher power transfers are possible over longer distances using fewer lines with HVDC transmission than with ac transmission. Typical HVDC lines utilize a bipolar configuration with two independent poles, one at a positive voltage and the other at a negative voltage with respect to ground. Bipolar HVDC lines are comparable to a double circuit ac line since they can operate at half power with one pole out of service but require only one-third the number of insulated sets of conductors as a double circuit ac line. Automatic restarts from temporary dc line fault clearing sequences are routine even for generator outlet transmission. No synchro-checking is required as for automatic reclosures following ac line faults since the dc restarts do not expose turbine generator units to high risk of transient torque amplification from closing into faults or across high phase angles. The controllability of HVDC links offer firm transmission capacity without limitation due to network congestion or loop flow on parallel paths. Controllability allows the HVDC to “leap-frog” multiple “choke-points” or bypass sequential path limits in the ac network. Therefore, the utilization of HVDC links is usually higher than that for extra high voltage ac transmission, lowering the transmission cost per MWh. This controllability can also be very beneficial for the parallel transmission since, by eliminating loop flow, it frees up this transmission capacity for its intended purpose of serving intermediate load and providing an outlet for local generation.

Whenever long-distance transmission is discussed, the concept of “break-even distance”

frequently arises. This is where the savings in line costs offset the higher converter station costs. A bipolar HVDC line uses only two insulated sets of conductors rather than three. This results in narrower rights-of-way, smaller transmission towers, and lower line losses than with ac lines of comparable capacity. A rough approximation of the savings in line construction is 30%.

Although break-even distance is influenced by the costs of right-of-way and line construction with a typical value of 500 km, the concept itself is misleading because in many cases more ac lines are needed to deliver the same power over the same distance due to system stability limitations. Furthermore, the long-distance ac lines usually require intermediate switching stations and reactive power compensation. This can increase the substation costs for ac transmission to the point where it is comparable to that for HVDC transmission.

For example, the generator outlet transmission alternative for the ± 250 -kV, 500-MW Square Butte Project was two 345-kV series-compensated ac transmission lines. The 12,600-MW Itaipu project has half its power delivered on three 800-kV series-compensated ac lines (three circuits) and the other half delivered on two ± 600 -kV bipolar HVDC lines (four circuits). Similarly, the ± 500 -kV, 1,600-MW Intermountain Power Project (IPP) ac alternative comprised two 500-kV ac lines. The IPP takes advantage of the double-circuit nature of the bipolar line and includes a 100% short-term and 50% continuous monopolar overload. The first 6,000-MW stage of the transmission for the Three Gorges Project in China would have required 5×500 -kV ac lines as opposed to $2 \times \pm 500$ -kV, 3,000-MW bipolar HVDC lines.

Table I contains an economic comparison of capital costs and losses for different ac and dc transmission alternatives for a hypothetical 750-mile (1200-km), 3,000-MW transmission system. The long transmission distance requires intermediate substations or switching stations and shunt reactors for the ac alternatives. The long distance and heavy power transfer, nearly twice the surge-impedance loading on the 500-kV ac alternatives, require a high level of series compensation. These ac station costs are included in the cost estimates for the ac alternatives.

It is interesting to compare the economics for transmission to that of transporting an equivalent amount of energy using other transport methods, in this case using rail transportation of sub-bituminous western coal with a heat content of 8,500 Btu/lb (19.8 MJ/kg) to support a 3,000-MW base load power plant with heat rate of 8,500 Btu/kWh (9 MJ/kWh) operating at an 85% load factor. The rail route is assumed to be longer than the more direct transmission

route; i.e., 900 miles (1400 km). Each unit train is comprised of 100 cars each carrying 100 tons (90 tonnes) of coal. The plant requires three unit trains per day. The annual coal transportation costs are about US\$560 million per year at an assumed rate of US\$50/ton (\$55/tonne). This works out to be US\$186 kW/year and US\$25 per MWh. The annual diesel fuel consumed in the process is in excess of 20 million gallons (76 million Liters) at 500 net ton-miles per gallon (193 net tonne-km per liter). The rail transportation costs are subject to escalation and congestion whereas the transmission costs are fixed. Furthermore, transmission is the only way to deliver remote renewable resources.

UNDERGROUND AND SUBMARINE CABLE TRANSMISSION

Unlike the case for ac cables, there is no physical restriction limiting the distance or power level for HVDC underground or submarine cables. Underground cables can be used on shared rights-of-way with other utilities without impacting reliability concerns over use of common corridors. For underground or submarine cable systems there is considerable savings in installed cable costs and cost of losses when using HVDC transmission. Depending on the power level to be transmitted, these savings can offset the higher converter station costs at distances of 40 km or more. Furthermore, there is a drop-off in cable capacity with ac transmission over distance due to its reactive component of charging current since cables have higher capacitances and lower inductances than ac overhead lines. Although this can be compensated by intermediate shunt compensation for underground cables at increased expense, it is not practical to do so for submarine cables.

For a given cable conductor area, the line losses with HVDC cables can be about half those of ac cables. This is due to ac cables requiring more conductors (three phases), carrying the reactive component of current, skin-effect, and induced currents in the cable sheath and armor.

With a cable system, the need to balance unequal loadings or the risk of postcontingency overloads often necessitates use of a series-connected reactors or phase shifting transformers. These potential problems do not exist with a controlled HVDC cable system.

Extruded HVDC cables with prefabricated joints used with VSC-based transmission are lighter, more flexible, and easier to splice than the mass-impregnated oil-paper cables (MINDs) used for conventional HVDC transmission, thus making them more conducive for land cable applications where transport limitations and extra splicing

TABLE I Comparative costs of HVDC and EHV AC transmission alternatives

Alternative	DC Alternatives				AC Alternatives				Hybrid AC/DC Alternative		
	+ 500 Kv Bipole	2 × +500 Kv 2 bipoles	+600 Kv Bipole	+800 Kv Bipole	500 kV 2 Single Ckt	500 kV Double Ckt	765 kV 2 Singl Ckt	+500 kV Bipole	500 kV Single Ckt	Total AC + DC	
Capital Cost											
Rated Power (MW)	3000	4000	3000	3000	3000	3000	3000	3000	1500	4500	
Station costs including reactive compensation (M\$)	\$420	\$680	\$465	\$510	\$542	\$542	\$630	\$420	\$302	\$722	
Transmission line cost (M\$/mile)*	\$1.60	\$1.60	\$1.80	\$1.95	\$2.00	\$3.20	\$2.80	\$1.60	\$2.00	\$2,700	
Distance in miles*	750	1,500	750	750	1,500	750	1,500	750	750	1,500	
Transmission Line Cost (M\$)	\$1,200	\$2,400	\$1,350	\$1,463	\$3,000	\$2,400	\$4,200	\$1,200	\$1,500	\$2,700	
Total Cost (M\$)	\$1,620	\$3,080	\$1,815	\$1,973	\$3,542	\$2,942	\$4,830	\$1,620	\$1,802	\$3,422	
Annual Payment, 30 years @ 10%	\$172	\$327	\$193	\$209	\$376	\$312	\$512	\$172	\$191	\$363	
Cost per kW-Yr	\$57.28	\$81.68	\$64.18	\$69.75	\$125.24	\$104.03	\$170.77	\$57.28	\$127.40	\$80.66	
Cost per MWh @ 85%											
Utilization Factor	\$7.69	\$10.97	\$8.62	\$9.37	\$16.82	\$13.97	\$22.93	\$7.69	\$17.11	\$10.83	
Losses @ full load	193	134	148	103	208	208	139	106	48	154	
Losses at full load in %	6.44%	3.35%	4.93%	3.43%	6.93%	6.93%	4.62%	5.29%	4.79%	5.12%	
Capitalized cost of losses @ \$1500 kW (M\$)	\$246	\$171	\$188	\$131	\$265	\$265	\$177	\$135	\$61	\$196	
Parameters:											
Interest rate %			10%								
Capitalized cost of losses \$/kW			\$1,500								
Note:											
AC current assumes 94% pf											
Full load converter station losses = 9.75% per station											
Total substation losses (transformers, reactors) assumed = 0.5% of rated power											

* 1 mile = 1.6 km

costs can drive up installation costs. The lower-cost cable installations made possible by the extruded HVDC cables and prefabricated joints makes long-distance underground transmission economically feasible for use in areas with rights-of-way constraints or subject to permitting difficulties or delays with overhead lines.

ASYNCHRONOUS TIES

With HVDC transmission systems, interconnections can be made between asynchronous networks for more economic or reliable system operation. The asynchronous interconnection allows interconnections of mutual benefit while providing a buffer between the two systems. Often these interconnections use back-to-back converters with no transmission line. Asynchronous HVDC links act as an effective “firewall” against propagation of cascading outages in one network from passing to another network.

Many asynchronous interconnections exist in North America between the Eastern and Western interconnected systems, between the Electric Reliability Council of Texas (ERCOT) and its neighbors, [e.g., Mexico and the Southwest Power Pool (SPP)], and between Quebec and its neighbors (e.g., New England and the Maritimes). The August 2003 Northeast blackout provides an example of the “firewall” against cascading outages provided by asynchronous interconnections. As the outage expanded and propagated around the lower Great Lakes and through Ontario and New York, it stopped at the asynchronous interface with Quebec. Quebec was unaffected; the weak ac interconnections between New York and New England tripped, but the HVDC links from Quebec continued to deliver power to New England.

Regulators try to eliminate “seams” in electrical networks because of their potential restriction on power markets. Electrical “seams,” however, serve as natural points of separation by acting as “shear-pins,” thereby reducing the impact of large-scale system disturbances. Asynchronous ties can eliminate market “seams” while retaining natural points of separation.

Interconnections between asynchronous networks are often at the periphery of the respective systems where the networks tend to be weak relative to the desired power transfer. Higher power transfers can be achieved with improved voltage stability in weak system applications using CCCs. The dynamic voltage support and improved voltage stability offered by VSC-based converters permits even higher power transfers

without as much need for ac system reinforcement. VSCs do not suffer commutation failures, allowing fast recoveries from nearby ac faults. Economic power schedules that reverse power direction can be made without any restrictions since there is no minimum power or current restrictions.

OFFSHORE TRANSMISSION

Self-commutation, dynamic voltage control, and black-start capability allow compact VSC HVDC transmission to serve isolated loads on islands or offshore production platforms over long-distance submarine cables. This capability can eliminate the need for running expensive local generation or provide an outlet for offshore generation such as that from wind. The VSCs can operate at variable frequency to more efficiently drive large compressor or pumping loads using high-voltage motors. Figure 11 shows the Troll A production platform in the North Sea where power to drive compressors is delivered from shore to reduce the higher carbon emissions and higher O&M costs associated with less efficient platform-based generation.

Large remote wind generation arrays require a collector system, reactive power support, and outlet transmission. Transmission for wind generation must often traverse scenic or environmentally sensitive areas or bodies of water. Many of the better wind sites with higher capacity factors are located offshore. VSC-based HVDC transmission allows efficient use of long-distance land or submarine cables and provides reactive support to the wind generation complex. Figure 12 shows a design for an

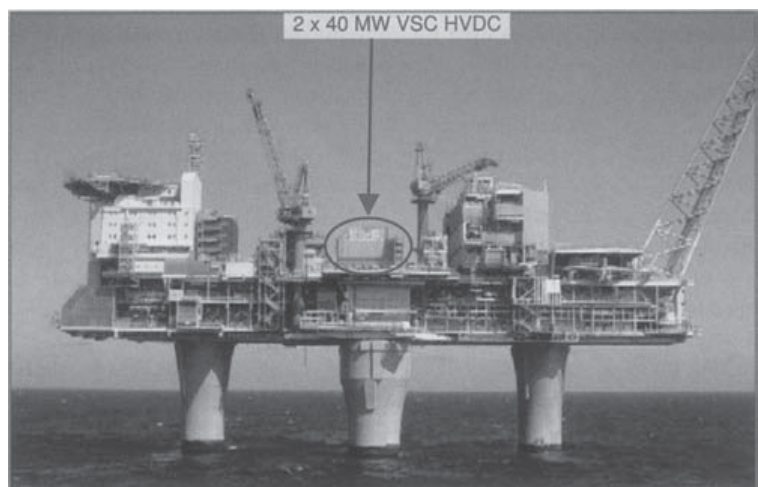


Figure 11
VSC power supply to Troll A production platform

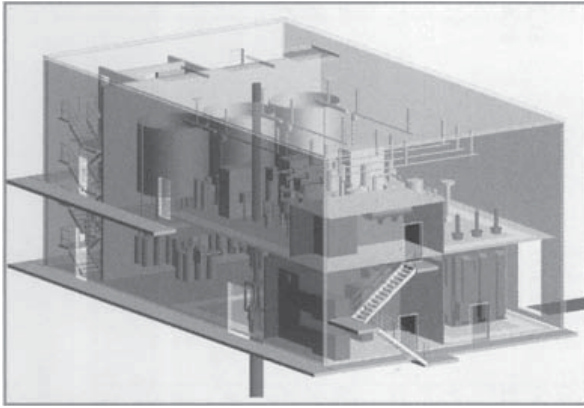


Figure 12
VSC converter for offshore wind generation

offshore converter station designed to transmit power from offshore wind generation.

MULTITERMINAL SYSTEMS

Most HVDC systems are for point-to-point transmission with a converter station at each end. The use of intermediate taps is rare. Conventional HVDC transmission uses voltage polarity reversal to reverse the power direction. Polarity reversal requires no special switching arrangement for a two-terminal system where both terminals reverse polarity by control action with no switching to reverse power direction. Special dc-side switching arrangements are needed for polarity reversal in a multi-terminal system, however, where it may be desired to reverse the power direction at a tap while maintaining the same power direction on the remaining terminals. For a bipolar system this can be done by connecting the converter to the opposite pole. VSC HVDC transmission, however, reverses power through reversal of the current direction rather than voltage polarity. Thus, power can be reversed at an intermediate tap independently of the main power flow direction without switching to reverse voltage polarity.

POWER DELIVERY TO LARGE URBAN AREAS

Power supply for large cities depends on local generation and power import capability. Local generation is often older and less efficient than newer units located remotely. Often, however, the older, less-efficient units located near the city center must be dispatched out-of-merit because they must be run for voltage support or reliability due to

inadequate transmission. Air quality regulations may limit the availability of these units. New transmission into large cities is difficult to site due to right-of-way limitations and land-use constraints.

Compact VSC-based underground transmission circuits can be placed on existing dual-use rights-of-way to bring in power as well as to provide voltage support, allowing a more economical power supply without compromising reliability. The receiving terminal acts like a virtual generator delivering power and supplying voltage regulation and dynamic reactive power reserve. Stations are compact and housed mainly indoors, making siting in urban areas somewhat easier. Furthermore, the dynamic voltage support offered by the VSC can often increase the capability of the adjacent ac transmission.

SYSTEM CONFIGURATIONS AND OPERATING MODES

Figure 13 shows the different common system configurations and operating modes used for HVDC transmission. Monopolar systems are the simplest and least expensive systems for moderate power transfers since only two converters and one high-voltage insulated cable or line conductor are required. Such systems have been used with low-voltage electrode lines and sea electrodes to carry the return current in submarine cable crossings.

In some areas conditions are not conducive to monopolar earth or sea return. This could be the case in heavily congested areas, fresh water cable crossings, or areas with high earth resistivity. In such cases a metallic neutral- or low-voltage cable is used for the return path and the dc circuit uses a simple local ground connection for potential reference only. Back-to-back stations are used for interconnection of asynchronous networks and use ac lines to connect on either side. In such systems power transfer is limited by the relative capacities of the adjacent ac systems at the point of connection.

As an economic alternative to a monopolar system with metallic return, the midpoint of a 12-pulse converter can be connected to earth directly or through an impedance and two half-voltage cables or line conductors can be used. The converter is only operated in 12-pulse mode so there is never any stray earth current.

VSC-based HVDC transmission is usually arranged with a single converter connected pole-to-pole rather than pole-to-ground. The center point of the converter is connected to ground through a high impedance to provide a reference for the dc voltage. Thus, half the converter dc

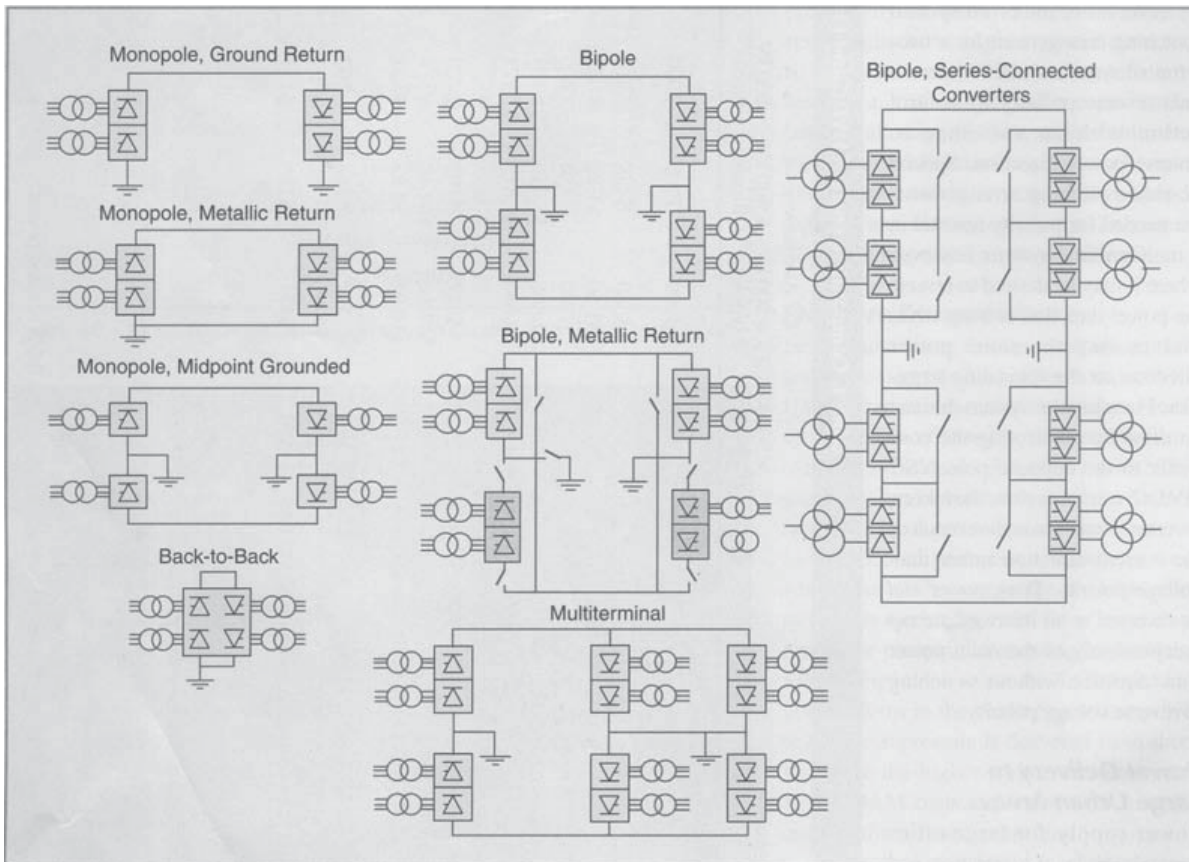


Figure 13
HVDC configurations and operating modes

voltage appears across the insulation on each of the two dc cables, one positive the other negative.

The most common configuration for modern overhead HVDC transmission lines is bipolar with a single 12-pulse converter for each pole at each terminal. This gives two independent dc circuits each capable of half capacity. For normal balanced operation there is no earth current. Monopolar earth return operation, often with overload capacity, can be used during outages of the opposite pole.

Earth return operation can be minimized during monopolar outages by using the opposite pole line for metallic return via pole/converter bypass switches at each end. This requires a metallic-return transfer breaker in the ground electrode line at one of the dc terminals to commutate the current from the relatively low resistance of the earth into that of the dc line conductor. Metallic return operation capability is provided for most dc transmission systems. This not only is effective during converter outages but also during line insulation failures where the remaining insulation strength is adequate to withstand the low resistive voltage drop in the metallic return path.

For very-high-power HVDC transmission, especially at dc voltages above ± 500 kV (i.e., ± 600 kV or ± 800 kV), series-connected converters can be used to reduce the energy unavailability for individual converter outages or partial line insulation failure. By using two series-connected converters per pole in a bipolar system, only one quarter of the transmission capacity is lost for a converter outage or if the line insulation for the affected pole is degraded to where it can only support half the rated dc line voltage. Operating in this mode also avoids the need to transfer to monopolar metallic return to limit the duration of emergency earth return.

STATION DESIGN AND LAYOUT

CONVENTIONAL HVDC

The converter station layout depends on a number of factors such as the dc system configuration (i.e., monopolar, bipolar, or back-to-back), ac filtering, and reactive power compensation requirements. The thyristor valves are air-insulated, water-cooled, and enclosed in a converter

building often referred to as a valve hall. For back-to-back ties with their characteristically low dc voltage, thyristor valves can be housed in prefabricated electrical enclosures, in which case a valve hall is not required.

To obtain a more compact station design and reduce the number of insulated high-voltage wall bushings, converter transformers are often placed adjacent to the valve hall with valve winding bushings protruding through the building walls for connection to the valves. Double or quadruple valve structures housing valve modules are used within the valve hall. Valve arresters are located immediately adjacent to the valves. Indoor motor-operated grounding switches are used for personnel safety during maintenance. Closed-loop valve cooling systems are used to circulate the cooling medium, deionized water or water-glycol mix, through the indoor thyristor valves with heat transfer to dry coolers located outdoors. Area requirements for conventional HVDC converter stations are influenced by the ac system voltage and reactive power compensation requirements where each individual bank rating may be limited by such system requirements as reactive power exchange and maximum voltage step on bank switching. The ac yard with filters and shunt compensation can take up as much as three quarters of the total area requirements of the converter station.

Figure 14 shows a typical arrangement for an HVDC converter station.

VSC-BASED HVDC

The transmission circuit consists of a bipolar two-wire HVDC system with converters connected pole-to-pole. DC capacitors are used to provide a stiff dc voltage source. The dc capacitors are grounded at their electrical center point to establish the earth reference potential for the transmission system. There is no earth return operation. The converters are coupled to the ac system through ac phase reactors and power transformers. Unlike most conventional HVDC systems, harmonic filters are located between the phase reactors and power transformers. Therefore, the transformers are exposed to no dc voltage stresses or harmonic loading, allowing use of ordinary power transformers. Figure 15 shows the station arrangement for a ± 150 -kV, 350 to 550-MW VSC converter station.

The IGBT valves used in VSC converters are comprised of series-connected IGBT positions. The IGBT is a hybrid device exhibiting the low forward drop of a bipolar transistor as a conducting device. Instead of the regular current-controlled base, the IGBT has a

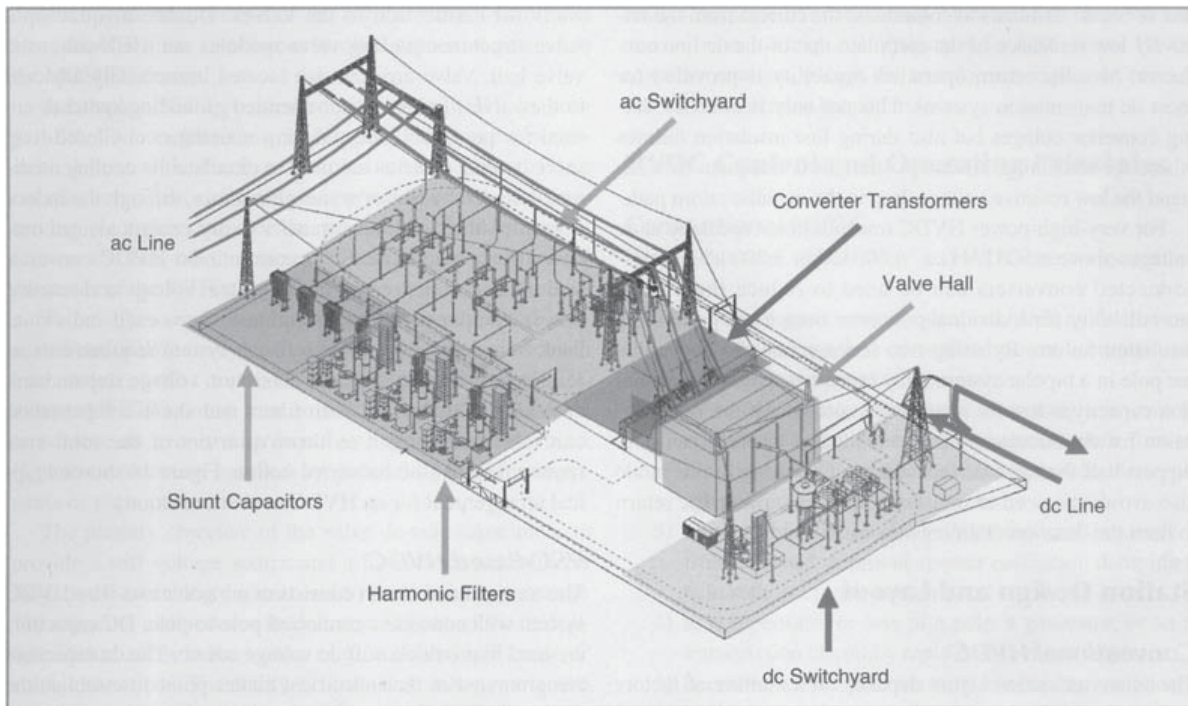


Figure 14
Monopolar HVDC converter station

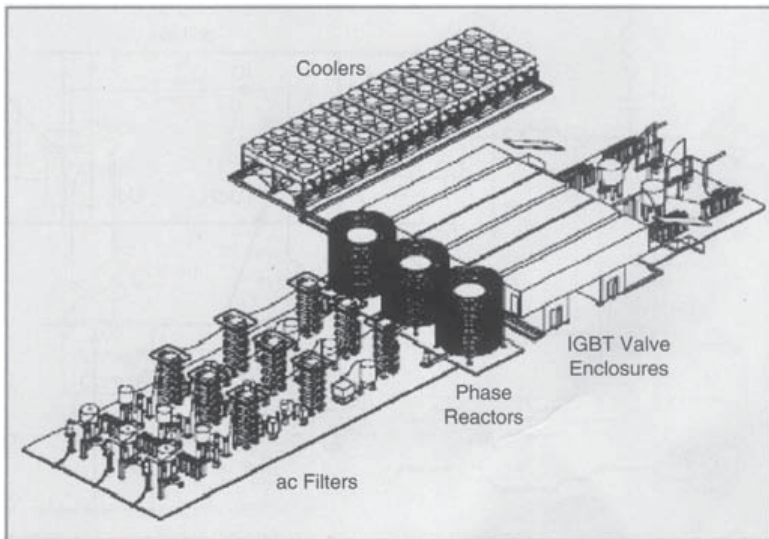


Figure 15
VSC HVDC converter station

voltage-controlled capacitive gate, as in the MOSFET device.

A complete IGBT position consists of an IGBT, an anti-parallel diode, a gate unit, a voltage divider, and a water-cooled heat sink. Each gate unit includes gate-driving circuits, surveillance circuits, and optical interface. The gate-driving electronics control the gate voltage and current at turn-on and turn-off to achieve optimal turn-on and turn-off processes of the IGBTs.

To be able to switch voltages higher than the rated voltage of one IGBT, many positions are connected in series in each valve similar to thyristors in conventional HVDC valves. All IGBTs must turn on and off at the same moment to achieve an evenly distributed voltage across the valve. Higher currents are handled by paralleling IGBT components or press packs.

The primary objective of the valve dc-side capacitor is to provide a stiff voltage source and a low-inductance path for the turn-off switching currents and to provide energy storage. The capacitor also reduces the harmonic ripple on the dc voltage. Disturbances in the system (e.g., ac faults) will cause dc voltage variations. The ability to limit these voltage variations depends on the size of the dc-side capacitor. Since the dc capacitors are used indoors, dry capacitors are used.

AC filters for VSC HVDC converters have smaller ratings than those for conventional converters and are not required for reactive power compensation. Therefore, these filters are always connected to the converter bus and not switched with transmission loading. All equipment

for VSC-based HVDC converter stations, except the transformer, high-side breaker, and valve coolers, is located indoors.

HVDC CONTROL AND OPERATING PRINCIPLES

CONVENTIONAL HVDC

The fundamental objectives of an HVDC control system are as follows:

- 1) to control basic system quantities such as dc line current, dc voltage, and transmitted power accurately and with sufficient speed of response
- 2) to maintain adequate commutation margin in inverter operation so that the valves can recover their forward blocking capability after conduction before their voltage polarity reverses
- 3) to control higher-level quantities such as frequency in isolated mode or provide power oscillation damping to help stabilize the ac network
- 4) to compensate for loss of a pole, a generator, or an ac transmission circuit by rapid readjustment of power
- 5) to ensure stable operation with reliable commutation in the presence of system disturbances
- 6) to minimize system losses and converter reactive power consumption
- 7) to ensure proper operation with fast and stable recoveries during ac system faults and disturbances.

For conventional HVDC transmission, one terminal sets the dc voltage level while the other terminal(s) regulates the (its) dc current by controlling its output voltage relative to that maintained by the voltage-setting terminal. Since the dc line resistance is low, large changes in current and hence power can be made with relatively small changes in firing angle (α). Two independent methods exist for controlling the converter dc output voltage. These are 1) by changing the ratio between the direct voltage and the ac voltage by varying the delay angle or 2) by changing the converter ac voltage via load tap changers (LTCs) on the converter transformer. Whereas the former method is rapid the latter method is slow due to the limited speed of response of the LTC. Use of high delay angles to achieve a larger dynamic range, however, increases the converter reactive power

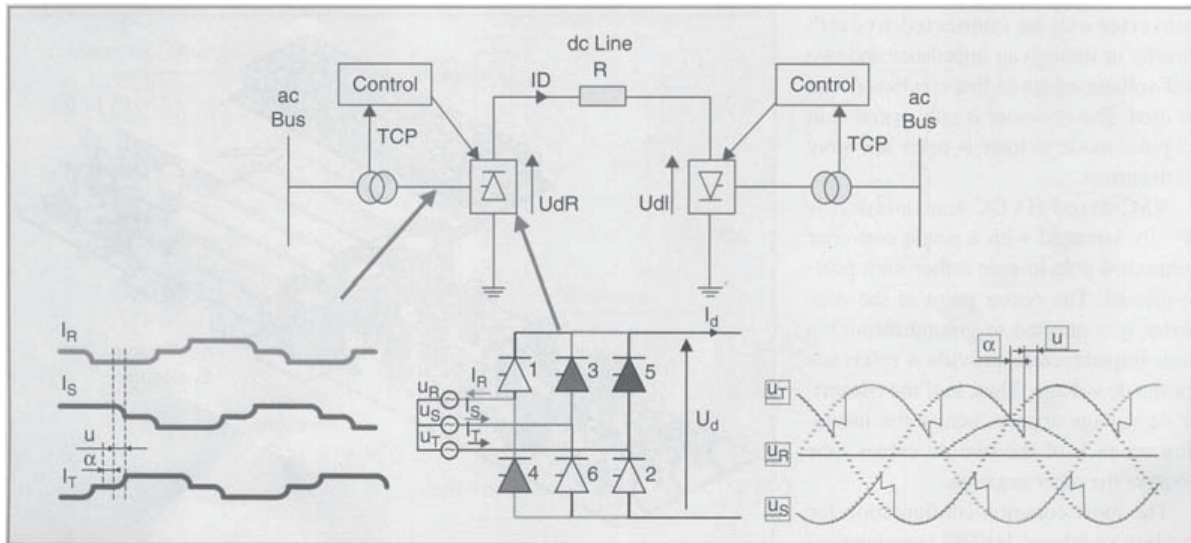


Figure 16
Conventional HVDC control

consumption. To minimize the reactive power demand while still providing adequate dynamic control range and commutation margin, the LTC is used at the rectifier terminal to keep the delay angle within its desired steady-state range (e.g., $13\text{--}18^\circ$) and at the inverter to keep the extinction angle within its desired range (e.g., $17\text{--}20^\circ$), if the angle is used for dc voltage control or to maintain rated dc voltage if operating in minimum commutation margin control mode. Figure 16 shows the characteristic transformer current and dc bridge voltage waveforms along with the controlled items U_d , I_d , and tap changer position (TCP).

VSC-BASED HVDC

Power can be controlled by changing the phase angle of the converter ac voltage with respect to the filter bus voltage, whereas the reactive power can be controlled by changing the magnitude of the fundamental component of the converter ac voltage with respect to the filter bus voltage. By controlling these two aspects of the converter voltage, operation in all four quadrants is possible. This means that the converter can be operated in the middle of its reactive power range near unity power factor to maintain dynamic reactive power reserve for contingency voltage support similar to a static var compensator. It also means that the real power transfer can be changed rapidly without altering the reactive power exchange with the ac network or waiting for switching of shunt compensation.

Being able to independently control ac voltage magnitude and phase relative to the system voltage allows use of separate active and reactive power control loops for HVDC system regulation. The active power control loop can be set to control either the active power or the dc-side voltage. In a dc link, one station will then be selected to control the active power while the other must be set to control the dc-side voltage. The reactive power control loop can be set to control either the reactive power or the ac-side voltage. Either of these two modes can be selected independently at either end of the dc link. Figure 17 shows the characteristic ac voltage waveforms before and after the ac filters along with the controlled items U_d , I_d , Q , and U_{ac} .

CONCLUSIONS

The favorable economics of long-distance bulk-power transmission with HVDC together with its controllability make it an interesting alternative or complement to ac transmission. The higher voltage levels, mature technology, and new converter designs have significantly increased the interest in HVDC transmission and expanded the range of applications.

FOR FURTHER READING

B. Jacobson, Y. Jiang-Hafner, P. Rey, and G. Asplund, "HVDC with voltage source converters and extruded

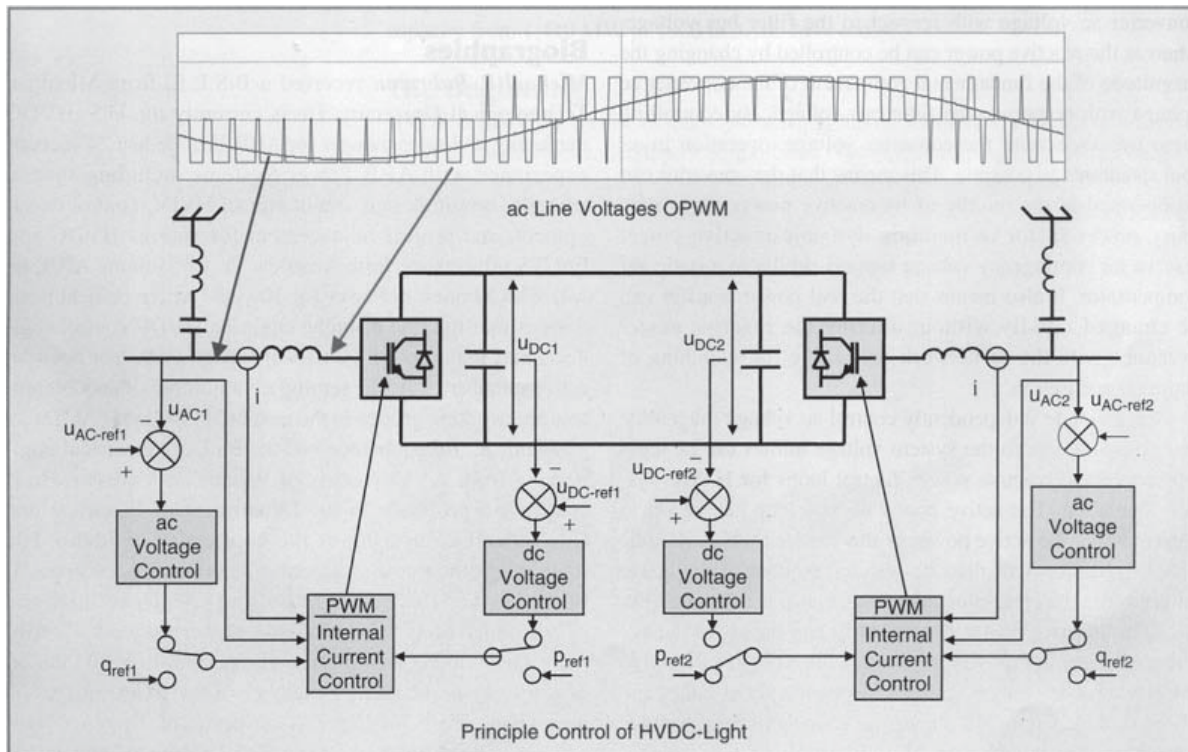


Figure 17
Control of VSC HVDC transmission

cables for up to ± 300 kV and 1000 MW,” in *Proc. CIGRÉ 2006*, Paris, France, pp. B4–105.

L. Ronstrom, B.D. Railing, J.J. Miller, P. Steckley, G. Moreau, P. Bard, and J. Lindberg, “Cross sound cable project second generation VSC technology for HVDC,” *Proc. CIGRÉ 2006*, Paris, France, pp. B4–102.

M. Bahrman, D. Dickinson, P. Fisher, and M. Stoltz, “The Rapid City Tie—New technology tames the East-West interconnection,” in *Proc. Minnesota Power Systems Conf.*, St. Paul, MN, Nov. 2004.

D. McCallum, G. Moreau, J. Primeau, D. Soulier, M. Bahrman, and B. Ekehov, “Multiterminal integration of the Nicolet Converter Station into the Quebec-New England Phase II transmission system,” in *Proc. CIGRÉ 1994*, Paris, France.

A. Ekstrom and G. Liss, “A refined HVDC control system,” *IEEE Trans. Power Systems*, vol. PAS-89, pp. 723–732, May–June 1970.

BIOGRAPHIES

Michael P. Bahrman received a B.S.E.E. from Michigan Technological University. He is currently the U.S. HVDC

marketing and sales manager for ABB Inc. He has 24 years of experience with ABB Power Systems including system analysis, system design, multiterminal HVDC control development, and project management for various HVDC and FACTS projects in North America. Prior to joining ABB, he was with Minnesota Power for 10 years where he held positions as transmission planning engineer, HVDC control engineer, and manager of system operations. He has been an active member of IEEE, serving on a number of subcommittees and working groups in the area of HVDC and FACTS.

Brian K. Johnson received the Ph.D. in electrical engineering from the University of Wisconsin-Madison. He is currently a professor in the Department of Electrical and Computer Engineering at the University of Idaho. His interests include power system protection and the application of power electronics to utility systems, security and survivability of ITS systems and power systems, distributed sensor and control networks, and real-time simulation of traffic systems. He is a member of the Board of Governors of the IEEE Intelligent Transportation Systems Society and the Administrative Committee of the IEEE Council on Superconductivity.

5.1

MEDIUM AND SHORT LINE APPROXIMATIONS

In this section, we present short and medium-length transmission-line approximations as a means of introducing $ABCD$ parameters. Some readers may prefer to start in Section 5.2, which presents the exact transmission-line equations.

It is convenient to represent a transmission line by the two-port network shown in Figure 5.1, where V_S and I_S are the sending-end voltage and current, and V_R and I_R are the receiving-end voltage and current.

The relation between the sending-end and receiving-end quantities can be written as

$$V_S = AV_R + BI_R \quad \text{volts} \quad (5.1.1)$$

$$I_S = CV_R + DI_R \quad \text{A} \quad (5.1.2)$$

or, in matrix format,

$$\begin{bmatrix} V_S \\ I_S \end{bmatrix} = \begin{bmatrix} A & B \\ C & D \end{bmatrix} \begin{bmatrix} V_R \\ I_R \end{bmatrix} \quad (5.1.3)$$

where A , B , C , and D are parameters that depend on the transmission-line constants R , L , C , and G . The $ABCD$ parameters are, in general, complex numbers. A and D are dimensionless. B has units of ohms, and C has units of siemens. Network theory texts [5] show that $ABCD$ parameters apply to linear, passive, bilateral two-port networks, with the following general relation:

$$AD - BC = 1 \quad (5.1.4)$$

The circuit in Figure 5.2 represents a short transmission line, usually applied to overhead 60-Hz lines less than 80 km long. Only the series resistance and reactance are included. The shunt admittance is neglected. The circuit applies to either single-phase or completely transposed three-phase lines operating under balanced conditions. For a completely transposed

FIGURE 5.1

Representation of two-port network

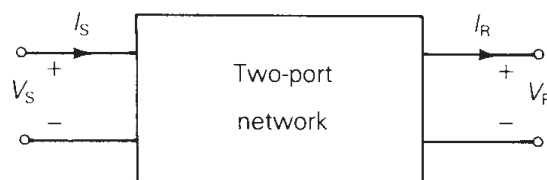
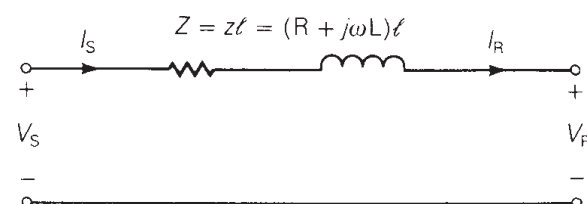


FIGURE 5.2

Short transmission line



three-phase line, Z is the series impedance, V_S and V_R are positive-sequence line-to-neutral voltages, and I_S and I_R are positive-sequence line currents.

To avoid confusion between total series impedance and series impedance per unit length, we use the following notation:

$$z = R + j\omega L \quad \Omega/\text{m}, \text{ series impedance per unit length}$$

$$y = G + j\omega C \quad \text{S}/\text{m}, \text{ shunt admittance per unit length}$$

$$Z = zl \quad \Omega, \text{ total series impedance}$$

$$Y = yl \quad \text{S}, \text{ total shunt admittance}$$

$$l = \text{line length} \quad \text{m}$$

Recall that shunt conductance G is usually neglected for overhead transmission.

The $ABCD$ parameters for the short line in Figure 5.2 are easily obtained by writing a KVL and KCL equation as

$$V_S = V_R + ZI_R \quad (5.1.5)$$

$$I_S = I_R \quad (5.1.6)$$

or, in matrix format,

$$\begin{bmatrix} V_S \\ I_S \end{bmatrix} = \begin{bmatrix} 1 & Z \\ 0 & 1 \end{bmatrix} \begin{bmatrix} V_R \\ I_R \end{bmatrix} \quad (5.1.7)$$

Comparing (5.1.7) and (5.1.3), the $ABCD$ parameters for a short line are

$$A = D = 1 \quad \text{per unit} \quad (5.1.8)$$

$$B = Z \quad \Omega \quad (5.1.9)$$

$$C = 0 \quad \text{S} \quad (5.1.10)$$

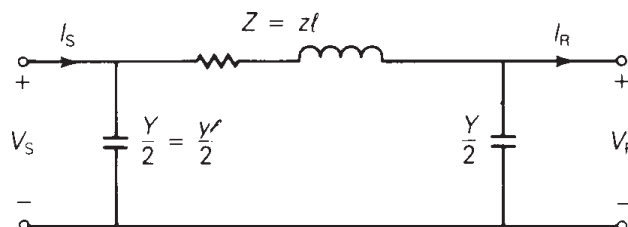
For medium-length lines, typically ranging from 80 to 250 km at 60 Hz, it is common to lump the total shunt capacitance and locate half at each end of the line. Such a circuit, called a *nominal π circuit*, is shown in Figure 5.3.

To obtain the $ABCD$ parameters of the nominal π circuit, note first that the current in the series branch in Figure 5.3 equals $I_R + \frac{V_R Y}{2}$. Then, writing a KVL equation,

$$\begin{aligned} V_S &= V_R + Z \left(I_R + \frac{V_R Y}{2} \right) \\ &= \left(1 + \frac{YZ}{2} \right) V_R + ZI_R \end{aligned} \quad (5.1.11)$$

FIGURE 5.3

Medium-length transmission line—nominal π circuit



Also, writing a KCL equation at the sending end,

$$I_S = I_R + \frac{V_R Y}{2} + \frac{V_S Y}{2} \quad (5.1.12)$$

Using (5.1.11) in (5.1.12),

$$\begin{aligned} I_S &= I_R + \frac{V_R Y}{2} + \left[\left(1 + \frac{YZ}{2} \right) V_R + Z I_R \right] \frac{Y}{2} \\ &= Y \left(1 + \frac{YZ}{4} \right) V_R + \left(1 + \frac{YZ}{2} \right) I_R \end{aligned} \quad (5.1.13)$$

Writing (5.1.11) and (5.1.13) in matrix format,

$$\begin{bmatrix} V_S \\ I_S \end{bmatrix} = \left[\begin{array}{c|c} \left(1 + \frac{YZ}{2} \right) & Z \\ \hline Y \left(1 + \frac{YZ}{4} \right) & \left(1 + \frac{YZ}{2} \right) \end{array} \right] \begin{bmatrix} V_R \\ I_R \end{bmatrix} \quad (5.1.14)$$

Thus, comparing (5.1.14) and (5.1.3)

$$A = D = 1 + \frac{YZ}{2} \quad \text{per unit} \quad (5.1.15)$$

$$B = Z \quad \Omega \quad (5.1.16)$$

$$C = Y \left(1 + \frac{YZ}{4} \right) \quad \text{S} \quad (5.1.17)$$

Note that for both the short and medium-length lines, the relation $AD - BC = 1$ is verified. Note also that since the line is the same when viewed from either end, $A = D$.

Figure 5.4 gives the $ABCD$ parameters for some common networks, including a series impedance network that approximates a short line and a π circuit that approximates a medium-length line. A medium-length line could also be approximated by the T circuit shown in Figure 5.4, lumping half of the series impedance at each end of the line. Also given are the $ABCD$ parameters for networks in series, which are conveniently obtained by multiplying the $ABCD$ matrices of the individual networks.

$ABCD$ parameters can be used to describe the variation of line voltage with line loading. *Voltage regulation* is the change in voltage at the receiving end of the line when the load varies from no-load to a specified full load at a specified power factor, while the sending-end voltage is held constant. Expressed in percent of full-load voltage,

$$\text{percent VR} = \frac{|V_{\text{RNL}}| - |V_{\text{RFL}}|}{|V_{\text{RFL}}|} \times 100 \quad (5.1.18)$$

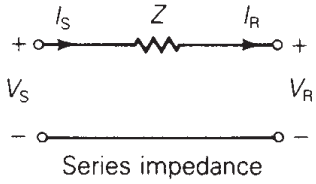
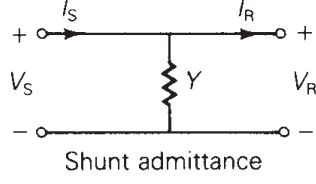
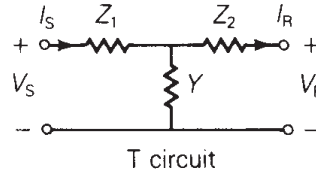
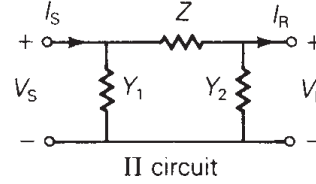
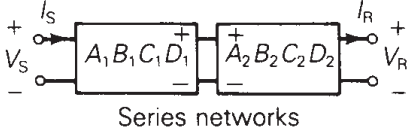
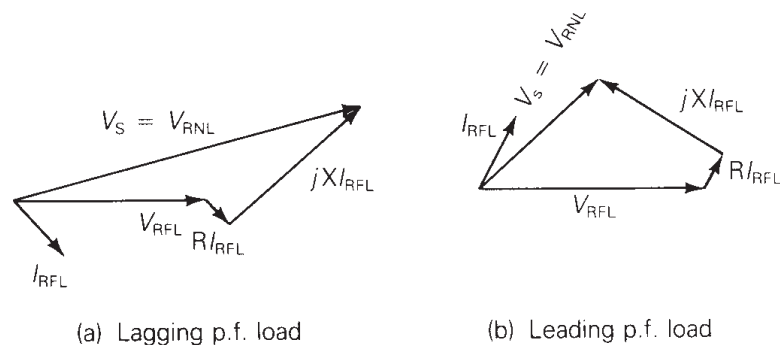
Circuit	ABCD Matrix
 <p>Series impedance</p>	$\begin{bmatrix} 1 & Z \\ 0 & 1 \end{bmatrix}$
 <p>Shunt admittance</p>	$\begin{bmatrix} 1 & 0 \\ Y & 1 \end{bmatrix}$
 <p>T circuit</p>	$\begin{bmatrix} (1 + YZ_1) & (Z_1 + Z_2 + YZ_1Z_2) \\ Y & (1 + YZ_2) \end{bmatrix}$
 <p>II circuit</p>	$\begin{bmatrix} (1 + Y_2Z) & Z \\ (Y_1 + Y_2 + Y_1Y_2Z) & (1 + Y_1Z) \end{bmatrix}$
 <p>Series networks</p>	$\begin{bmatrix} A_1 & B_1 \\ C_1 & D_1 \end{bmatrix} \begin{bmatrix} A_2 & B_2 \\ C_2 & D_2 \end{bmatrix} = \begin{bmatrix} (A_1A_2 + B_1C_2) & (A_1B_2 + B_1D_2) \\ (C_1A_2 + D_1C_2) & (C_1B_2 + D_1D_2) \end{bmatrix}$

FIGURE 5.4 ABCD parameters of common networks

FIGURE 5.5

Phasor diagrams for a short transmission line



where percent VR is the percent voltage regulation, $|V_{RNL}|$ is the magnitude of the no-load receiving-end voltage, and $|V_{RFL}|$ is the magnitude of the full-load receiving-end voltage.

The effect of load power factor on voltage regulation is illustrated by the phasor diagrams in Figure 5.5 for short lines. The phasor diagrams are graphical representations of (5.1.5) for lagging and leading power factor loads. Note that, from (5.1.5) at no-load, $I_{RNL} = 0$ and $V_S = V_{RNL}$ for a short line. As shown, the higher (worse) voltage regulation occurs for the lagging p.f. load, where V_{RNL} exceeds V_{RFL} by the larger amount. A smaller or even negative voltage regulation occurs for the leading p.f. load. In general, the no-load voltage is, from (5.1.1), with $I_{RNL} = 0$,

$$V_{RNL} = \frac{V_S}{A} \quad (5.1.19)$$

which can be used in (5.1.18) to determine voltage regulation.

In practice, transmission-line voltages decrease when heavily loaded and increase when lightly loaded. When voltages on EHV lines are maintained within $\pm 5\%$ of rated voltage, corresponding to about 10% voltage regulation, unusual operating problems are not encountered. Ten percent voltage regulation for lower voltage lines including transformer-voltage drops is also considered good operating practice.

In addition to voltage regulation, line loadability is an important issue. Three major line-loading limits are: (1) the thermal limit, (2) the voltage-drop limit, and (3) the steady-state stability limit.

The maximum temperature of a conductor determines its thermal limit. Conductor temperature affects the conductor sag between towers and the loss of conductor tensile strength due to annealing. If the temperature is too high, prescribed conductor-to-ground clearances may not be met, or the elastic limit of the conductor may be exceeded such that it cannot shrink to its original length when cooled. Conductor temperature depends on the current magnitude and its time duration, as well as on ambient temperature, wind velocity, and conductor surface conditions. Appendix Tables A.3 and A.4 give approximate current-carrying capacities of copper and ACSR conductors. The loadability of short transmission lines (less than 80 km in length for 60-Hz overhead lines) is usually determined by the conductor thermal limit or by ratings of line terminal equipment such as circuit breakers.

For longer line lengths (up to 300 km), line loadability is often determined by the voltage-drop limit. Although more severe voltage drops may be tolerated in some cases, a heavily loaded line with $V_R/V_S \geq 0.95$ is usually considered safe operating practice. For line lengths over 300 km, steady-state stability becomes a limiting factor. Stability, discussed in Section 5.4, refers to the ability of synchronous machines on either end of a line to remain in synchronism.

EXAMPLE 5.1 ABCD parameters and the nominal π circuit: medium-length line

A three-phase, 60-Hz, completely transposed 345-kV, 200-km line has two 795,000-cmil (403-mm^2) 26/2 ACSR conductors per bundle and the following positive-sequence line constants:

$$z = 0.032 + j0.35 \quad \Omega/\text{km}$$

$$y = j4.2 \times 10^{-6} \quad \text{S}/\text{km}$$

Full load at the receiving end of the line is 700 MW at 0.99 p.f. leading and at 95% of rated voltage. Assuming a medium-length line, determine the following:

- $ABCD$ parameters of the nominal π circuit
- Sending-end voltage V_S , current I_S , and real power P_S
- Percent voltage regulation
- Thermal limit, based on the approximate current-carrying capacity listed in Table A.4
- Transmission-line efficiency at full load

SOLUTION

- a. The total series impedance and shunt admittance values are

$$Z = zl = (0.032 + j0.35)(200) = 6.4 + j70 = 70.29/\underline{84.78^\circ} \quad \Omega$$

$$Y = yl = (j4.2 \times 10^{-6})(200) = 8.4 \times 10^{-4}/\underline{90^\circ} \quad \text{S}$$

From (5.1.15)–(5.1.17),

$$\begin{aligned} A = D &= 1 + (8.4 \times 10^{-4}/\underline{90^\circ})(70.29/\underline{84.78^\circ})(\frac{1}{2}) \\ &= 1 + 0.02952/\underline{174.78^\circ} \\ &= 0.9706 + j0.00269 = 0.9706/\underline{0.159^\circ} \quad \text{per unit} \end{aligned}$$

$$B = Z = 70.29/\underline{84.78^\circ} \quad \Omega$$

$$\begin{aligned} C &= (8.4 \times 10^{-4}/\underline{90^\circ})(1 + 0.01476/\underline{174.78^\circ}) \\ &= (8.4 \times 10^{-4}/\underline{90^\circ})(0.9853 + j0.00134) \\ &= 8.277 \times 10^{-4}/\underline{90.08^\circ} \quad \text{S} \end{aligned}$$

- b. The receiving-end voltage and current quantities are

$$V_R = (0.95)(345) = 327.8 \quad \text{kV}_{LL}$$

$$V_R = \frac{327.8}{\sqrt{3}}/\underline{0^\circ} = 189.2/\underline{0^\circ} \quad \text{kV}_{LN}$$

$$I_R = \frac{700/\underline{\cos^{-1} 0.99}}{(\sqrt{3})(0.95 \times 345)(0.99)} = 1.246/\underline{8.11^\circ} \quad \text{kA}$$

From (5.1.1) and (5.1.2), the sending-end quantities are

$$\begin{aligned} V_S &= (0.9706/\underline{0.159^\circ})(189.2/\underline{0^\circ}) + (70.29/\underline{84.78^\circ})(1.246/\underline{8.11^\circ}) \\ &= 183.6/\underline{0.159^\circ} + 87.55/\underline{92.89^\circ} \\ &= 179.2 + j87.95 = 199.6/\underline{26.14^\circ} \quad \text{kV}_{LN} \end{aligned}$$

$$V_S = 199.6\sqrt{3} = 345.8 \text{ kV}_{LL} \approx 1.00 \text{ per unit}$$

$$\begin{aligned} I_S &= (8.277 \times 10^{-4} / 90.08^\circ)(189.2 / 0^\circ) + (0.9706 / 0.159^\circ)(1.246 / 8.11^\circ) \\ &= 0.1566 / 90.08^\circ + 1.209 / 8.27^\circ \\ &= 1.196 + j0.331 = 1.241 / 15.5^\circ \text{ kA} \end{aligned}$$

and the real power delivered to the sending end is

$$\begin{aligned} P_S &= (\sqrt{3})(345.8)(1.241) \cos(26.14^\circ - 15.5^\circ) \\ &= 730.5 \text{ MW} \end{aligned}$$

c. From (5.1.19), the no-load receiving-end voltage is

$$V_{RNL} = \frac{V_S}{A} = \frac{345.8}{0.9706} = 356.3 \text{ kV}_{LL}$$

and, from (5.1.18),

$$\text{percent VR} = \frac{356.3 - 327.8}{327.8} \times 100 = 8.7\%$$

d. From Table A.4, the approximate current-carrying capacity of two 795,000-cmil (403-mm²) 26/2 ACSR conductors is $2 \times 0.9 = 1.8$ kA.

e. The full-load line losses are $P_S - P_R = 730.5 - 700 = 30.5$ MW and the full-load transmission efficiency is

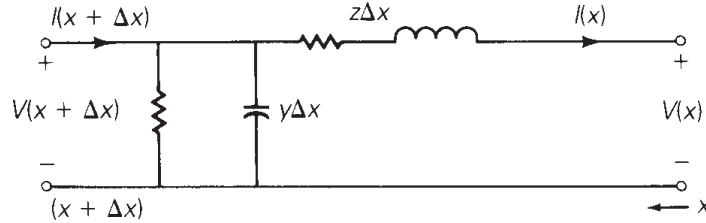
$$\text{percent EFF} = \frac{P_R}{P_S} \times 100 = \frac{700}{730.5} \times 100 = 95.8\%$$

Since $V_S = 1.00$ per unit, the full-load receiving-end voltage of 0.95 per unit corresponds to $V_R/V_S = 0.95$, considered in practice to be about the lowest operating voltage possible without encountering operating problems. Thus, for this 345-kV 200-km uncompensated line, voltage drop limits the full-load current to 1.246 kA at 0.99 p.f. leading, well below the thermal limit of 1.8 kA. ■

5.2

TRANSMISSION-LINE DIFFERENTIAL EQUATIONS

The line constants R , L , and C are derived in Chapter 4 as per-length values having units of Ω/m , H/m , and F/m . They are not lumped, but rather are uniformly distributed along the length of the line. In order to account for the distributed nature of transmission-line constants, consider the circuit shown in Figure 5.6, which represents a line section of length Δx . $V(x)$ and $I(x)$ denote the voltage and current at position x , which is measured in meters from the right, or receiving end of the line. Similarly, $V(x + \Delta x)$ and $I(x + \Delta x)$ denote the voltage and current at position $(x + \Delta x)$. The circuit constants are

FIGURE 5.6Transmission-line section of length Δx 

$$z = R + j\omega L \quad \Omega/\text{m} \quad (5.2.1)$$

$$y = G + j\omega C \quad \text{S}/\text{m} \quad (5.2.2)$$

where G is usually neglected for overhead 60-Hz lines. Writing a KVL equation for the circuit

$$V(x + \Delta x) = V(x) + (z\Delta x)I(x) \quad \text{volts} \quad (5.2.3)$$

Rearranging (5.2.3),

$$\frac{V(x + \Delta x) - V(x)}{\Delta x} = zI(x) \quad (5.2.4)$$

and taking the limit as Δx approaches zero,

$$\frac{dV(x)}{dx} = zI(x) \quad (5.2.5)$$

Similarly, writing a KCL equation for the circuit,

$$I(x + \Delta x) = I(x) + (y\Delta x)V(x + \Delta x) \quad \text{A} \quad (5.2.6)$$

Rearranging,

$$\frac{I(x + \Delta x) - I(x)}{\Delta x} = yV(x) \quad (5.2.7)$$

and taking the limit as Δx approaches zero,

$$\frac{dI(x)}{dx} = yV(x) \quad (5.2.8)$$

Equations (5.2.5) and (5.2.8) are two linear, first-order, homogeneous differential equations with two unknowns, $V(x)$ and $I(x)$. We can eliminate $I(x)$ by differentiating (5.2.5) and using (5.2.8) as follows:

$$\frac{d^2V(x)}{dx^2} = z \frac{dI(x)}{dx} = zyV(x) \quad (5.2.9)$$

or

$$\frac{d^2V(x)}{dx^2} - zyV(x) = 0 \quad (5.2.10)$$

Equation (5.2.10) is a linear, second-order, homogeneous differential equation with one unknown, $V(x)$. By inspection, its solution is

$$V(x) = A_1 e^{\gamma x} + A_2 e^{-\gamma x} \quad \text{volts} \quad (5.2.11)$$

where A_1 and A_2 are integration constants and

$$\gamma = \sqrt{zy} \quad \text{m}^{-1} \quad (5.2.12)$$

γ , whose units are m^{-1} , is called the *propagation constant*. By inserting (5.2.11) and (5.2.12) into (5.2.10), the solution to the differential equation can be verified.

Next, using (5.2.11) in (5.2.5),

$$\frac{dV(x)}{dx} = \gamma A_1 e^{\gamma x} - \gamma A_2 e^{-\gamma x} = zI(x) \quad (5.2.13)$$

Solving for $I(x)$,

$$I(x) = \frac{A_1 e^{\gamma x} - A_2 e^{-\gamma x}}{z/\gamma} \quad (5.2.14)$$

Using (5.2.12), $z/\gamma = z/\sqrt{zy} = \sqrt{z/y}$, (5.2.14) becomes

$$I(x) = \frac{A_1 e^{\gamma x} - A_2 e^{-\gamma x}}{Z_c} \quad (5.2.15)$$

where

$$Z_c = \sqrt{\frac{z}{y}} \quad \Omega \quad (5.2.16)$$

Z_c , whose units are Ω , is called the *characteristic impedance*.

Next, the integration constants A_1 and A_2 are evaluated from the boundary conditions. At $x = 0$, the receiving end of the line, the receiving-end voltage and current are

$$V_R = V(0) \quad (5.2.17)$$

$$I_R = I(0) \quad (5.2.18)$$

Also, at $x = 0$, (5.2.11) and (5.2.15) become

$$V_R = A_1 + A_2 \quad (5.2.19)$$

$$I_R = \frac{A_1 - A_2}{Z_c} \quad (5.2.20)$$

Solving for A_1 and A_2 ,

$$A_1 = \frac{V_R + Z_c I_R}{2} \quad (5.2.21)$$

$$A_2 = \frac{V_R - Z_c I_R}{2} \quad (5.2.22)$$

Substituting A_1 and A_2 into (5.2.11) and (5.2.15),

$$V(x) = \left(\frac{V_R + Z_c I_R}{2} \right) e^{\gamma x} + \left(\frac{V_R - Z_c I_R}{2} \right) e^{-\gamma x} \quad (5.2.23)$$

$$I(x) = \left(\frac{V_R + Z_c I_R}{2Z_c} \right) e^{\gamma x} - \left(\frac{V_R - Z_c I_R}{2Z_c} \right) e^{-\gamma x} \quad (5.2.24)$$

Rearranging (5.2.23) and (5.2.24),

$$V(x) = \left(\frac{e^{\gamma x} + e^{-\gamma x}}{2} \right) V_R + Z_c \left(\frac{e^{\gamma x} - e^{-\gamma x}}{2} \right) I_R \quad (5.2.25)$$

$$I(x) = \frac{1}{Z_c} \left(\frac{e^{\gamma x} - e^{-\gamma x}}{2} \right) V_R + \left(\frac{e^{\gamma x} + e^{-\gamma x}}{2} \right) I_R \quad (5.2.26)$$

Recognizing the hyperbolic functions \cosh and \sinh ,

$$V(x) = \cosh(\gamma x) V_R + Z_c \sinh(\gamma x) I_R \quad (5.2.27)$$

$$I(x) = \frac{1}{Z_c} \sinh(\gamma x) V_R + \cosh(\gamma x) I_R \quad (5.2.28)$$

Equations (5.2.27) and (5.2.28) give the $ABCD$ parameters of the distributed line. In matrix format,

$$\begin{bmatrix} V(x) \\ I(x) \end{bmatrix} = \begin{bmatrix} A(x) & B(x) \\ C(x) & D(x) \end{bmatrix} \begin{bmatrix} V_R \\ I_R \end{bmatrix} \quad (5.2.29)$$

where

$$A(x) = D(x) = \cosh(\gamma x) \quad \text{per unit} \quad (5.2.30)$$

$$B(x) = Z_c \sinh(\gamma x) \quad \Omega \quad (5.2.31)$$

$$C(x) = \frac{1}{Z_c} \sinh(\gamma x) \quad \text{S} \quad (5.2.32)$$

Equation (5.2.29) gives the current and voltage at any point x along the line in terms of the receiving-end voltage and current. At the sending end, where $x = l$, $V(l) = V_S$ and $I(l) = I_S$. That is,

$$\begin{bmatrix} V_S \\ I_S \end{bmatrix} = \begin{bmatrix} A & B \\ C & D \end{bmatrix} \begin{bmatrix} V_R \\ I_R \end{bmatrix} \quad (5.2.33)$$

where

$$A = D = \cosh(\gamma l) \quad \text{per unit} \quad (5.2.34)$$

$$B = Z_c \sinh(\gamma l) \quad \Omega \quad (5.2.35)$$

$$C = \frac{1}{Z_c} \sinh(\gamma l) \quad \text{S} \quad (5.2.36)$$

Equations (5.2.34)–(5.2.36) give the $ABCD$ parameters of the distributed line. In these equations, the propagation constant γ is a complex quantity with real and imaginary parts denoted α and β . That is,

$$\gamma = \alpha + j\beta \quad \text{m}^{-1} \tag{5.2.37}$$

The quantity γl is dimensionless. Also

$$e^{\gamma l} = e^{(\alpha + j\beta)l} = e^{\alpha l} e^{j\beta l} = e^{\alpha l} \underline{\angle \beta l} \tag{5.2.38}$$

Using (5.2.38) the hyperbolic functions \cosh and \sinh can be evaluated as follows:

$$\cosh(\gamma l) = \frac{e^{\gamma l} + e^{-\gamma l}}{2} = \frac{1}{2}(e^{\alpha l} \underline{\angle \beta l} + e^{-\alpha l} \underline{\angle -\beta l}) \tag{5.2.39}$$

and

$$\sinh(\gamma l) = \frac{e^{\gamma l} - e^{-\gamma l}}{2} = \frac{1}{2}(e^{\alpha l} \underline{\angle \beta l} - e^{-\alpha l} \underline{\angle -\beta l}) \tag{5.2.40}$$

Alternatively, the following identities can be used:

$$\cosh(\alpha l + j\beta l) = \cosh(\alpha l) \cos(\beta l) + j \sinh(\alpha l) \sin(\beta l) \tag{5.2.41}$$

$$\sinh(\alpha l + j\beta l) = \sinh(\alpha l) \cos(\beta l) + j \cosh(\alpha l) \sin(\beta l) \tag{5.2.42}$$

Note that in (5.2.39)–(5.2.42), the dimensionless quantity βl is in radians, not degrees.

The $ABCD$ parameters given by (5.2.34)–(5.2.36) are exact parameters valid for any line length. For accurate calculations, these equations must be used for overhead 60-Hz lines longer than 250 km. The $ABCD$ parameters derived in Section 5.1 are approximate parameters that are more conveniently used for hand calculations involving short and medium-length lines. Table 5.1 summarizes the $ABCD$ parameters for short, medium, long, and lossless (see Section 5.4) lines.

TABLE 5.1

Summary: Transmission-line $ABCD$ parameters

Parameter	$A = D$	B	C
Units	per Unit	Ω	S
Short line (less than 80 km)	1	Z	0
Medium line—nominal π circuit (80 to 250 km)	$1 + \frac{YZ}{2}$	Z	$Y \left(1 + \frac{YZ}{4} \right)$
Long line—equivalent π circuit (more than 250 km)	$\cosh(\gamma \ell) = 1 + \frac{Y'Z'}{2}$	$Z_c \sinh(\gamma \ell) = Z'$	$(1/Z_c) \sinh(\gamma \ell) = Y' \left(1 + \frac{Y'Z'}{4} \right)$
Lossless line ($R = G = 0$)	$\cos(\beta \ell)$	$jZ_c \sin(\beta \ell)$	$\frac{j \sin(\beta \ell)}{Z_c}$

EXAMPLE 5.2 Exact ABCD parameters: long line

A three-phase 765-kV, 60-Hz, 300-km, completely transposed line has the following positive-sequence impedance and admittance:

$$z = 0.0165 + j0.3306 = 0.3310/\underline{87.14^\circ} \quad \Omega/\text{km}$$

$$y = j4.674 \times 10^{-6} \quad \text{S/km}$$

Assuming positive-sequence operation, calculate the exact $ABCD$ parameters of the line. Compare the exact B parameter with that of the nominal π circuit.

SOLUTION From (5.2.12) and (5.2.16):

$$\begin{aligned} Z_c &= \sqrt{\frac{0.3310/\underline{87.14^\circ}}{4.674 \times 10^{-6}/\underline{90^\circ}}} = \sqrt{7.082 \times 10^4/\underline{-2.86^\circ}} \\ &= 266.1/\underline{-1.43^\circ} \quad \Omega \end{aligned}$$

and

$$\begin{aligned} \gamma l &= \sqrt{(0.3310/\underline{87.14^\circ})(4.674 \times 10^{-6}/\underline{90^\circ})} \times (300) \\ &= \sqrt{1.547 \times 10^{-6}/\underline{177.14^\circ}} \times (300) \\ &= 0.3731/\underline{88.57^\circ} = 0.00931 + j0.3730 \quad \text{per unit} \end{aligned}$$

From (5.2.38),

$$\begin{aligned} e^{\gamma l} &= e^{0.00931} e^{+j0.3730} = 1.0094/\underline{0.3730} \quad \text{radians} \\ &= 0.9400 + j0.3678 \end{aligned}$$

and

$$\begin{aligned} e^{-\gamma l} &= e^{-0.00931} e^{-j0.3730} = 0.9907/\underline{-0.3730} \quad \text{radians} \\ &= 0.9226 - j0.3610 \end{aligned}$$

Then, from (5.2.39) and (5.2.40),

$$\begin{aligned} \cosh(\gamma l) &= \frac{(0.9400 + j0.3678) + (0.9226 - j0.3610)}{2} \\ &= 0.9313 + j0.0034 = 0.9313/\underline{0.209^\circ} \\ \sinh(\gamma l) &= \frac{(0.9400 + j0.3678) - (0.9226 - j0.3610)}{2} \\ &= 0.0087 + j0.3644 = 0.3645/\underline{88.63^\circ} \end{aligned}$$

Finally, from (5.2.34)–(5.2.36),

$$A = D = \cosh(\gamma l) = 0.9313/\underline{0.209^\circ} \text{ per unit}$$

$$B = (266.1/\underline{-1.43^\circ})(0.3645/\underline{88.63^\circ}) = 97.0/\underline{87.2^\circ} \ \Omega$$

$$C = \frac{0.3645/\underline{88.63^\circ}}{266.1/\underline{-1.43^\circ}} = 1.37 \times 10^{-3}/\underline{90.06^\circ} \text{ S}$$

Using (5.1.16), the B parameter for the nominal π circuit is

$$B_{\text{nominal } \pi} = Z = (0.3310/\underline{87.14^\circ})(300) = 99.3/\underline{87.14^\circ} \ \Omega$$

which is 2% larger than the exact value. ■

5.3

EQUIVALENT π CIRCUIT

Many computer programs used in power system analysis and design assume circuit representations of components such as transmission lines and transformers (see the power-flow program described in Chapter 6 as an example). It is therefore convenient to represent the terminal characteristics of a transmission line by an equivalent circuit instead of its $ABCD$ parameters.

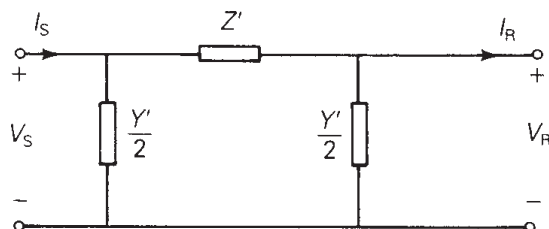
The circuit shown in Figure 5.7 is called an *equivalent π circuit*. It is identical in structure to the nominal π circuit of Figure 5.3, except that Z' and Y' are used instead of Z and Y . Our objective is to determine Z' and Y' such that the equivalent π circuit has the same $ABCD$ parameters as those of the distributed line, (5.2.34)–(5.2.36). The $ABCD$ parameters of the equivalent π circuit, which has the same structure as the nominal π , are

$$A = D = 1 + \frac{Y'Z'}{2} \text{ per unit} \quad (5.3.1)$$

$$B = Z' \ \Omega \quad (5.3.2)$$

FIGURE 5.7

Transmission-line
equivalent π circuit



$$Z' = Z_c \sinh(\gamma \ell) = ZF_1 = Z \frac{\sinh(\gamma \ell)}{\gamma \ell}$$

$$\frac{Y'}{2} = \frac{\tanh(\gamma \ell / 2)}{Z_c} = \frac{Y}{2} F_2 = \frac{Y \tanh(\gamma \ell / 2)}{(\gamma \ell / 2)}$$

$$C = Y' \left(1 + \frac{Y'Z'}{4} \right) \text{ S} \quad (5.3.3)$$

where we have replaced Z and Y in (5.1.15)–(5.1.17) with Z' and Y' in (5.3.1)–(5.3.3). Equating (5.3.2) to (5.2.35),

$$Z' = Z_c \sinh(\gamma l) = \sqrt{\frac{\bar{z}}{y}} \sinh(\gamma l) \quad (5.3.4)$$

Rewriting (5.3.4) in terms of the nominal π circuit impedance $Z = zl$,

$$\begin{aligned} Z' &= zl \left[\sqrt{\frac{\bar{z}}{y}} \frac{\sinh(\gamma l)}{zl} \right] = zl \left[\frac{\sinh(\gamma l)}{\sqrt{\bar{z}y}l} \right] \\ &= ZF_1 \quad \Omega \end{aligned} \quad (5.3.5)$$

where

$$F_1 = \frac{\sinh(\gamma l)}{\gamma l} \quad \text{per unit} \quad (5.3.6)$$

Similarly, equating (5.3.1) to (5.2.34),

$$\begin{aligned} 1 + \frac{Y'Z'}{2} &= \cosh(\gamma l) \\ \frac{Y'}{2} &= \frac{\cosh(\gamma l) - 1}{Z'} \end{aligned} \quad (5.3.7)$$

Using (5.3.4) and the identity $\tanh\left(\frac{\gamma l}{2}\right) = \frac{\cosh(\gamma l) - 1}{\sinh(\gamma l)}$, (5.3.7) becomes

$$\frac{Y'}{2} = \frac{\cosh(\gamma l) - 1}{Z_c \sinh(\gamma l)} = \frac{\tanh(\gamma l/2)}{Z_c} = \frac{\tanh(\gamma l/2)}{\sqrt{\frac{\bar{z}}{y}}} \quad (5.3.8)$$

Rewriting (5.3.8) in terms of the nominal π circuit admittance $Y = yl$,

$$\begin{aligned} \frac{Y'}{2} &= \frac{yl}{2} \left[\frac{\tanh(\gamma l/2)}{\sqrt{\frac{\bar{z}}{y}} \frac{yl}{2}} \right] = \frac{yl}{2} \left[\frac{\tanh(\gamma l/2)}{\sqrt{\bar{z}y}l/2} \right] \\ &= \frac{Y}{2} F_2 \quad \text{S} \end{aligned} \quad (5.3.9)$$

where

$$F_2 = \frac{\tanh(\gamma l/2)}{\gamma l/2} \quad \text{per unit} \quad (5.3.10)$$

Equations (5.3.6) and (5.3.10) give the correction factors F_1 and F_2 to convert Z and Y for the nominal π circuit to Z' and Y' for the equivalent π circuit.

EXAMPLE 5.3 Equivalent π circuit: long line

Compare the equivalent and nominal π circuits for the line in Example 5.2.

SOLUTION For the nominal π circuit,

$$Z = zl = (0.3310/87.14^\circ)(300) = 99.3/87.14^\circ \quad \Omega$$

$$\frac{Y}{2} = \frac{yl}{2} = \left(\frac{j4.674 \times 10^{-6}}{2} \right) (300) = 7.011 \times 10^{-4}/90^\circ \quad \text{S}$$

From (5.3.6) and (5.3.10), the correction factors are

$$F_1 = \frac{0.3645/88.63^\circ}{0.3731/88.57^\circ} = 0.9769/0.06^\circ \quad \text{per unit}$$

$$\begin{aligned} F_2 &= \frac{\tanh(\gamma l/2)}{\gamma l/2} = \frac{\cosh(\gamma l) - 1}{(\gamma l/2) \sinh(\gamma l)} \\ &= \frac{0.9313 + j0.0034 - 1}{\left(\frac{0.3731}{2} / 88.57^\circ \right) (0.3645/88.63^\circ)} \\ &= \frac{-0.0687 + j0.0034}{0.06800/177.20^\circ} \\ &= \frac{0.06878/177.17^\circ}{0.06800/177.20^\circ} = 1.012/-0.03^\circ \quad \text{per unit} \end{aligned}$$

Then, from (5.3.5) and (5.3.9), for the equivalent π circuit,

$$Z' = (99.3/87.14^\circ)(0.9769/0.06^\circ) = 97.0/87.2^\circ \quad \Omega$$

$$\begin{aligned} \frac{Y'}{2} &= (7.011 \times 10^{-4}/90^\circ)(1.012/-0.03^\circ) = 7.095 \times 10^{-4}/89.97^\circ \quad \text{S} \\ &= 3.7 \times 10^{-7} + j7.095 \times 10^{-4} \quad \text{S} \end{aligned}$$

Comparing these nominal and equivalent π circuit values, Z' is about 2% smaller than Z , and $Y'/2$ is about 1% larger than $Y/2$. Although the circuit values are approximately the same for this line, the equivalent π circuit should be used for accurate calculations involving long lines. Note the small shunt conductance, $G' = 3.7 \times 10^{-7}$ S, introduced in the equivalent π circuit. G' is often neglected. ■

5.4

LOSSLESS LINES

In this section, we discuss the following concepts for lossless lines: surge impedance, $ABCD$ parameters, equivalent π circuit, wavelength, surge impedance loading, voltage profiles, and steady-state stability limit.

When line losses are neglected, simpler expressions for the line parameters are obtained and the above concepts are more easily understood. Since transmission and distribution lines for power transfer generally are designed to have low losses, the equations and concepts developed here can be used for quick and reasonably accurate hand calculations leading to seat-of-the-pants analyses and to initial designs. More accurate calculations can then be made with computer programs for follow-up analysis and design.

SURGE IMPEDANCE

For a lossless line, $R = G = 0$, and

$$z = j\omega L \quad \Omega/\text{m} \quad (5.4.1)$$

$$y = j\omega C \quad \text{S}/\text{m} \quad (5.4.2)$$

From (5.2.12) and (5.2.16),

$$Z_c = \sqrt{\frac{z}{y}} = \sqrt{\frac{j\omega L}{j\omega C}} = \sqrt{\frac{L}{C}} \quad \Omega \quad (5.4.3)$$

and

$$\gamma = \sqrt{zy} = \sqrt{(j\omega L)(j\omega C)} = j\omega\sqrt{LC} = j\beta \quad \text{m}^{-1} \quad (5.4.4)$$

where

$$\beta = \omega\sqrt{LC} \quad \text{m}^{-1} \quad (5.4.5)$$

The characteristic impedance $Z_c = \sqrt{L/C}$, commonly called *surge* impedance for a lossless line, is pure real—that is, resistive. The propagation constant $\gamma = j\beta$ is pure imaginary.

ABCD PARAMETERS

The $ABCD$ parameters are, from (5.2.30)–(5.2.32),

$$\begin{aligned} A(x) = D(x) &= \cosh(\gamma x) = \cosh(j\beta x) \\ &= \frac{e^{j\beta x} + e^{-j\beta x}}{2} = \cos(\beta x) \quad \text{per unit} \end{aligned} \quad (5.4.6)$$

$$\sinh(\gamma x) = \sinh(j\beta x) = \frac{e^{j\beta x} - e^{-j\beta x}}{2} = j \sin(\beta x) \quad \text{per unit} \quad (5.4.7)$$

$$B(x) = Z_c \sinh(\gamma x) = jZ_c \sin(\beta x) = j\sqrt{\frac{L}{C}} \sin(\beta x) \quad \Omega \quad (5.4.8)$$

$$C(x) = \frac{\sinh(\gamma x)}{Z_c} = \frac{j \sin(\beta x)}{\sqrt{\frac{L}{C}}} \quad \text{S} \quad (5.4.9)$$

$A(x)$ and $D(x)$ are pure real; $B(x)$ and $C(x)$ are pure imaginary.

A comparison of lossless versus lossy $ABCD$ parameters is shown in Table 5.1.

EQUIVALENT π CIRCUIT

For the equivalent π circuit, using (5.3.4),

$$Z' = jZ_c \sin(\beta l) = jX' \quad \Omega \quad (5.4.10)$$

or, from (5.3.5) and (5.3.6),

$$Z' = (j\omega Ll) \left(\frac{\sin(\beta l)}{\beta l} \right) = jX' \quad \Omega \quad (5.4.11)$$

Also, from (5.3.9) and (5.3.10),

$$\begin{aligned} \frac{Y'}{2} &= \frac{Y \tanh(j\beta l/2)}{j\beta l/2} = \frac{Y \sinh(j\beta l/2)}{(j\beta l/2) \cosh(j\beta l/2)} \\ &= \left(\frac{j\omega Cl}{2} \right) \frac{j \sin(\beta l/2)}{(j\beta l/2) \cos(\beta l/2)} = \left(\frac{j\omega Cl}{2} \right) \frac{\tan(\beta l/2)}{\beta l/2} \\ &= \left(\frac{j\omega C'l}{2} \right) \text{ S} \end{aligned} \quad (5.4.12)$$

Z' and Y' are both pure imaginary. Also, for βl less than π radians, Z' is pure inductive and Y' is pure capacitive. Thus the equivalent π circuit for a lossless line, shown in Figure 5.8, is also lossless.

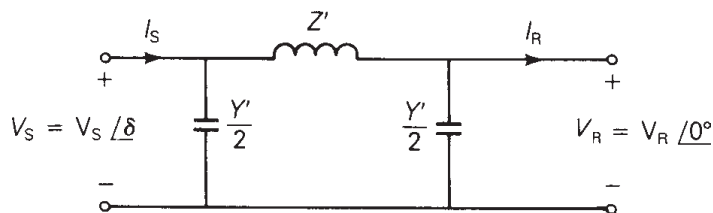
WAVELENGTH

A *wavelength* is the distance required to change the phase of the voltage or current by 2π radians or 360° . For a lossless line, using (5.2.29),

$$\begin{aligned} V(x) &= A(x)V_R + B(x)I_R \\ &= \cos(\beta x)V_R + jZ_c \sin(\beta x)I_R \end{aligned} \quad (5.4.13)$$

FIGURE 5.8

Equivalent π circuit for a lossless line ($\beta\ell$ less than π)



$$Z' = (j\omega L\ell) \left(\frac{\sin \beta\ell}{\beta\ell} \right) = jX' \quad \Omega$$

$$\frac{Y'}{2} = \left(\frac{j\omega C\ell}{2} \right) \frac{\tan(\beta\ell/2)}{(\beta\ell/2)} = \frac{j\omega C'\ell}{2} \text{ S}$$

and

$$\begin{aligned} I(x) &= C(x)V_R + D(x)I_R \\ &= \frac{j \sin(\beta x)}{Z_c} V_R + \cos(\beta x)I_R \end{aligned} \quad (5.4.14)$$

From (5.4.13) and (5.4.14), $V(x)$ and $I(x)$ change phase by 2π radians when $x = 2\pi/\beta$. Denoting wavelength by λ , and using (5.4.5),

$$\lambda = \frac{2\pi}{\beta} = \frac{2\pi}{\omega\sqrt{LC}} = \frac{1}{f\sqrt{LC}} \quad \text{m} \quad (5.4.15)$$

or

$$f\lambda = \frac{1}{\sqrt{LC}} \quad (5.4.16)$$

We will show in Chapter 12 that the term $(1/\sqrt{LC})$ in (5.4.16) is the velocity of propagation of voltage and current waves along a lossless line. For overhead lines, $(1/\sqrt{LC}) \approx 3 \times 10^8$ m/s, and for $f = 60$ Hz, (5.4.14) gives

$$\lambda \approx \frac{3 \times 10^8}{60} = 5 \times 10^6 \text{ m} = 5000 \text{ km}$$

Typical power-line lengths are only a small fraction of the above 60-Hz wavelength.

SURGE IMPEDANCE LOADING

Surge impedance loading (SIL) is the power delivered by a lossless line to a load resistance equal to the surge impedance $Z_c = \sqrt{L/C}$. Figure 5.9 shows a lossless line terminated by a resistance equal to its surge impedance. This line represents either a single-phase line or one phase-to-neutral of a balanced three-phase line. At SIL, from (5.4.13),

$$\begin{aligned} V(x) &= \cos(\beta x)V_R + jZ_c \sin(\beta x)I_R \\ &= \cos(\beta x)V_R + jZ_c \sin(\beta x)\left(\frac{V_R}{Z_c}\right) \\ &= (\cos \beta x + j \sin \beta x)V_R \\ &= e^{j\beta x} V_R \quad \text{volts} \end{aligned} \quad (5.4.17)$$

$$|V(x)| = |V_R| \quad \text{volts} \quad (5.4.18)$$

FIGURE 5.9

Lossless line terminated by its surge impedance

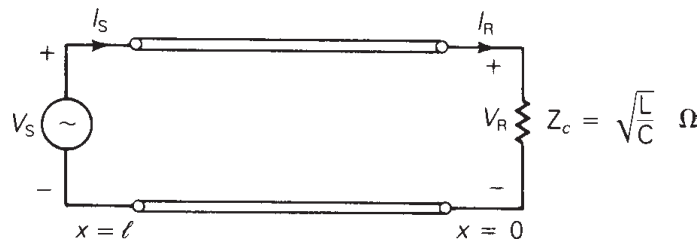


TABLE 5.2

V_{rated} (kV)	$Z_c = \sqrt{L/C}$ (Ω)	$\text{SIL} = V_{\text{rated}}^2 / Z_c$ (MW)
69	366–400	12–13
138	366–405	47–52
230	365–395	134–145
345	280–366	325–425
500	233–294	850–1075
765	254–266	2200–2300

Surge impedance and SIL values for typical 60-Hz overhead lines [1, 2] (Electric Power Research Institute (EPRI), EPRI AC Transmission Line Reference Book—200 kV and Above (Palo Alto, CA: EPRI, www.epri.com, December 2005); Westinghouse Electric Corporation, Electrical Transmission and Distribution Reference Book, 4th ed. (East Pittsburgh, PA, 1964))

Thus, at SIL, the voltage profile is flat. That is, the voltage magnitude at any point x along a lossless line at SIL is constant.

Also from (5.4.14) at SIL,

$$\begin{aligned}
 I(x) &= \frac{j \sin(\beta x)}{Z_c} V_R + (\cos \beta x) \frac{V_R}{Z_c} \\
 &= (\cos \beta x + j \sin \beta x) \frac{V_R}{Z_c} \\
 &= (e^{j\beta x}) \frac{V_R}{Z_c} \quad \text{A}
 \end{aligned} \tag{5.4.19}$$

Using (5.4.17) and (5.4.19), the complex power flowing at any point x along the line is

$$\begin{aligned}
 S(x) &= P(x) + jQ(x) = V(x)I^*(x) \\
 &= (e^{j\beta x} V_R) \left(\frac{e^{j\beta x} V_R}{Z_c} \right)^* \\
 &= \frac{|V_R|^2}{Z_c}
 \end{aligned} \tag{5.4.20}$$

Thus the real power flow along a lossless line at SIL remains constant from the sending end to the receiving end. The reactive power flow is zero.

At rated line voltage, the real power delivered, or SIL, is, from (5.4.20),

$$\text{SIL} = \frac{V_{\text{rated}}^2}{Z_c} \tag{5.4.21}$$

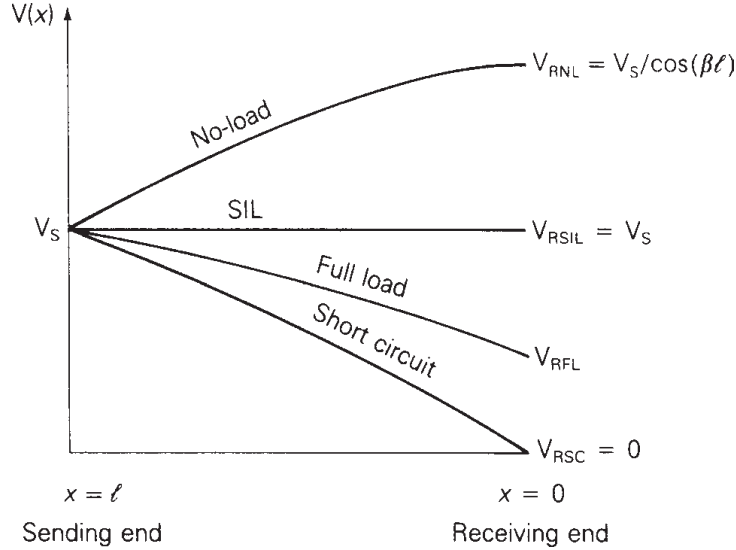
where rated voltage is used for a single-phase line and rated line-to-line voltage is used for the total real power delivered by a three-phase line. Table 5.2 lists surge impedance and SIL values for typical overhead 60-Hz three-phase lines.

VOLTAGE PROFILES

In practice, power lines are not terminated by their surge impedance. Instead, loadings can vary from a small fraction of SIL during light load conditions

FIGURE 5.10

Voltage profiles of an uncompensated lossless line with fixed sending-end voltage for line lengths up to a quarter wavelength



up to multiples of SIL, depending on line length and line compensation, during heavy load conditions. If a line is not terminated by its surge impedance, then the voltage profile is not flat. Figure 5.10 shows voltage profiles of lines with a fixed sending-end voltage magnitude V_S for line lengths l up to a quarter wavelength. This figure shows four loading conditions: (1) no-load, (2) SIL, (3) short circuit, and (4) full load, which are described as follows:

1. At no-load, $I_{RNL} = 0$ and (5.4.13) yields

$$V_{NL}(x) = (\cos \beta x) V_{RNL} \quad (5.4.22)$$

The no-load voltage increases from $V_S = (\cos \beta l) V_{RNL}$ at the sending end to V_{RNL} at the receiving end (where $x = 0$).

2. From (5.4.18), the voltage profile at SIL is flat.
3. For a short circuit at the load, $V_{RSC} = 0$ and (5.4.13) yields

$$V_{SC}(x) = (Z_c \sin \beta x) I_{RSC} \quad (5.4.23)$$

The voltage decreases from $V_S = (\sin \beta l) (Z_c I_{RSC})$ at the sending end to $V_{RSC} = 0$ at the receiving end.

4. The full-load voltage profile, which depends on the specification of full-load current, lies above the short-circuit voltage profile.

Figure 5.10 summarizes these results, showing a high receiving-end voltage at no-load and a low receiving-end voltage at full load. This voltage regulation problem becomes more severe as the line length increases. In Section 5.6, we discuss shunt compensation methods to reduce voltage fluctuations.

STEADY-STATE STABILITY LIMIT

The equivalent π circuit of Figure 5.8 can be used to obtain an equation for the real power delivered by a lossless line. Assume that the voltage magnitudes V_S and V_R at the ends of the line are held constant. Also, let δ denote the voltage-phase angle at the sending end with respect to the receiving end. From KVL, the receiving-end current I_R is

$$\begin{aligned} I_R &= \frac{V_S - V_R}{Z'} - \frac{Y'}{2} V_R \\ &= \frac{V_S e^{j\delta} - V_R}{jX'} - \frac{j\omega C'l}{2} V_R \end{aligned} \quad (5.4.24)$$

and the complex power S_R delivered to the receiving end is

$$\begin{aligned} S_R &= V_R I_R^* = V_R \left(\frac{V_S e^{j\delta} - V_R}{jX'} \right)^* + \frac{j\omega C'l}{2} V_R^2 \\ &= V_R \left(\frac{V_S e^{-j\delta} - V_R}{-jX'} \right) + \frac{j\omega Cl}{2} V_R^2 \\ &= \frac{jV_R V_S \cos \delta + V_R V_S \sin \delta - jV_R^2}{X'} + \frac{j\omega Cl}{2} V_R^2 \end{aligned} \quad (5.4.25)$$

The real power delivered is

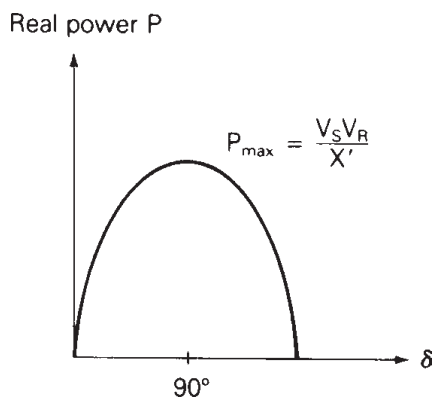
$$P = P_S = P_R = \operatorname{Re}(S_R) = \frac{V_R V_S}{X'} \sin \delta \quad \text{W} \quad (5.4.26)$$

Note that since the line is lossless, $P_S = P_R$.

Equation (5.4.26) is plotted in Figure 5.11. For fixed voltage magnitudes V_S and V_R , the phase angle δ increases from 0 to 90° as the real power delivered increases. The maximum power that the line can deliver, which occurs when $\delta = 90^\circ$, is given by

$$P_{\max} = \frac{V_S V_R}{X'} \quad \text{W} \quad (5.4.27)$$

FIGURE 5.11 Real power delivered by a lossless line versus voltage angle across the line



P_{\max} represents the theoretical *steady-state stability* limit of a lossless line. If an attempt were made to exceed this steady-state stability limit, then synchronous machines at the sending end would lose synchronism with those at the receiving end. Stability is further discussed in Chapter 13.

It is convenient to express the steady-state stability limit in terms of SIL. Using (5.4.10) in (5.4.26),

$$P = \frac{V_S V_R \sin \delta}{Z_c \sin \beta l} = \left(\frac{V_S V_R}{Z_c} \right) \frac{\sin \delta}{\sin \left(\frac{2\pi l}{\lambda} \right)} \quad (5.4.28)$$

Expressing V_S and V_R in per-unit of rated line voltage,

$$\begin{aligned} P &= \left(\frac{V_S}{V_{\text{rated}}} \right) \left(\frac{V_R}{V_{\text{rated}}} \right) \left(\frac{V_{\text{rated}}^2}{Z_c} \right) \frac{\sin \delta}{\sin \left(\frac{2\pi l}{\lambda} \right)} \\ &= V_{S,\text{p.u.}} V_{R,\text{p.u.}} (\text{SIL}) \frac{\sin \delta}{\sin \left(\frac{2\pi l}{\lambda} \right)} \quad \text{W} \end{aligned} \quad (5.4.29)$$

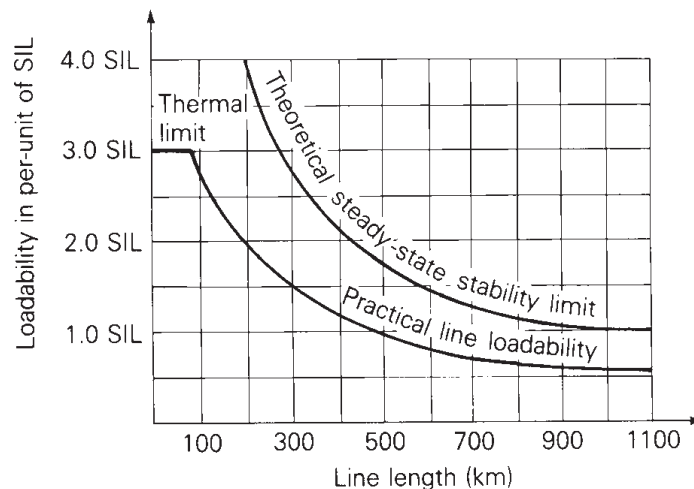
And for $\delta = 90^\circ$, the theoretical steady-state stability limit is

$$P_{\max} = \frac{V_{S,\text{p.u.}} V_{R,\text{p.u.}} (\text{SIL})}{\sin \left(\frac{2\pi l}{\lambda} \right)} \quad \text{W} \quad (5.4.30)$$

Equations (5.4.27)–(5.4.30) reveal two important factors affecting the steady-state stability limit. First, from (5.4.27), it increases with the square of the line voltage. For example, a doubling of line voltage enables a fourfold increase in maximum power flow. Second, it decreases with line length. Equation (5.4.30) is plotted in Figure 5.12 for $V_{S,\text{p.u.}} = V_{R,\text{p.u.}} = 1$, $\lambda = 5000$ km, and line lengths up to 1100 km. As shown, the theoretical steady-state stability limit decreases from 4(SIL) for a 200-km line to about 2(SIL) for a 400-km line.

FIGURE 5.12

Transmission-line loadability curve for 60-Hz overhead lines—no series or shunt compensation



EXAMPLE 5.4 Theoretical steady-state stability limit: long line

Neglecting line losses, find the theoretical steady-state stability limit for the 300-km line in Example 5.2. Assume a $266.1\text{-}\Omega$ surge impedance, a 5000-km wavelength, and $V_S = V_R = 765\text{ kV}$.

SOLUTION From (5.4.21),

$$\text{SIL} = \frac{(765)^2}{266.1} = 2199 \text{ MW}$$

From (5.4.30) with $l = 300\text{ km}$ and $\lambda = 5000\text{ km}$,

$$P_{\max} = \frac{(1)(1)(2199)}{\sin\left(\frac{2\pi \times 300}{5000}\right)} = (2.716)(2199) = 5974 \text{ MW}$$

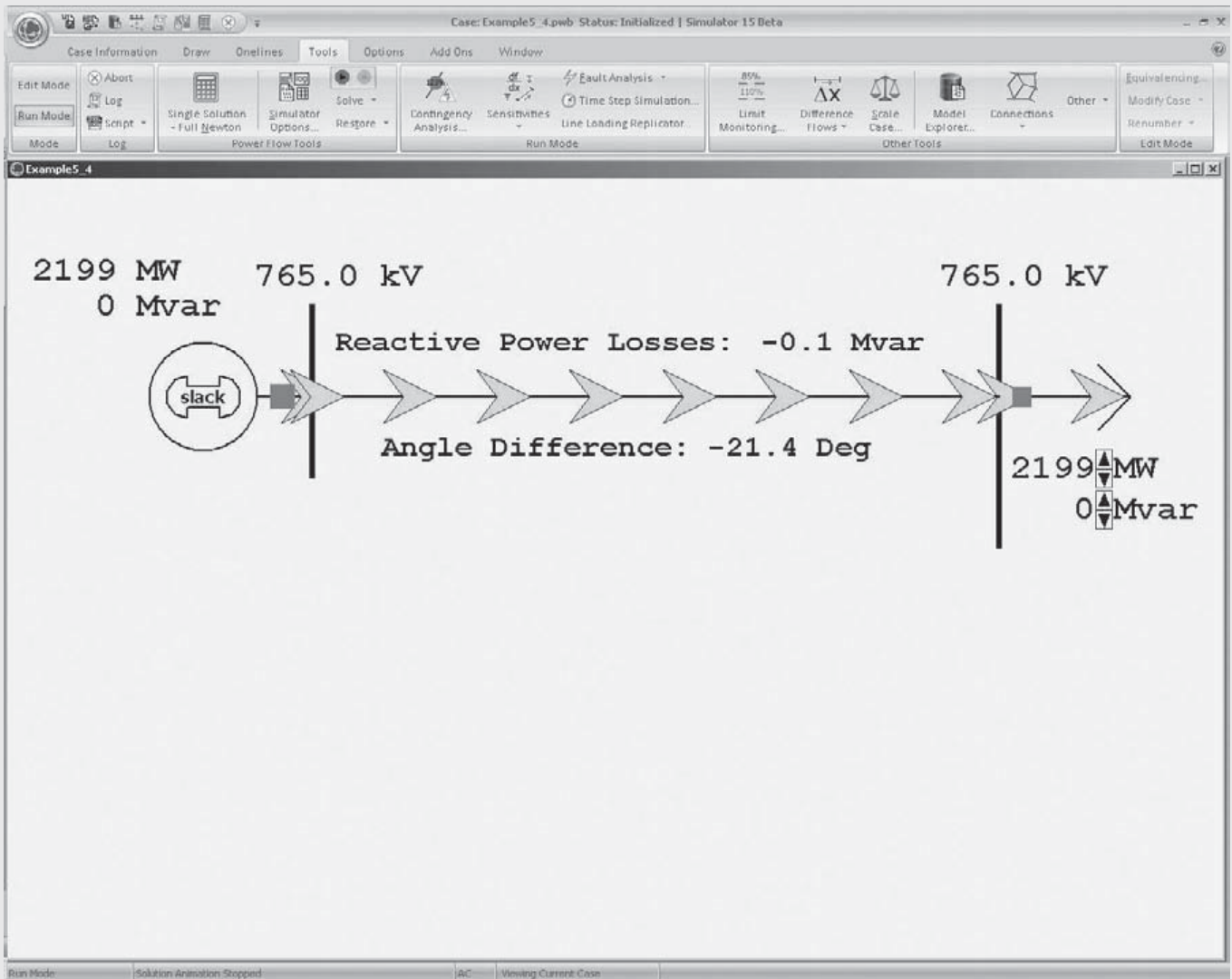


FIGURE 5.13 Screen for Example 5.4

Alternatively, from Figure 5.12, for a 300-km line, the theoretical steady-state stability limit is $(2.72)\text{SIL} = (2.72)(2199) = 5980 \text{ MW}$, about the same as the above result (see Figure 5.13).

Open PowerWorld Simulator case Example 5_4 and select **Tools Play** to see an animated view of this example. When the load on a line is equal to the SIL, the voltage profile across the line is flat and the line's net reactive power losses are zero. For loads above the SIL, the line consumes reactive power and the load's voltage magnitude is below the sending-end value. Conversely, for loads below the SIL, the line actually generates reactive power and the load's voltage magnitude is above the sending-end value. Use the load arrow button to vary the load to see the changes in the receiving-end voltage and the line's reactive power consumption. ■

5.5

MAXIMUM POWER FLOW

Maximum power flow, discussed in Section 5.4 for lossless lines, is derived here in terms of the $ABCD$ parameters for lossy lines. The following notation is used:

$$\begin{aligned} A &= \cosh(\gamma l) = A/\theta_A \\ B &= Z' = Z'/\theta_Z \\ V_S &= V_S/\delta \quad V_R = V_R/0^\circ \end{aligned}$$

Solving (5.2.33) for the receiving-end current,

$$I_R = \frac{V_S - AV_R}{B} = \frac{V_S e^{j\delta} - AV_R e^{j\theta_A}}{Z' e^{j\theta_Z}} \quad (5.5.1)$$

The complex power delivered to the receiving end is

$$\begin{aligned} S_R &= P_R + jQ_R = V_R I_R^* = V_R \left[\frac{V_S e^{j(\delta - \theta_Z)} - AV_R e^{j(\theta_A - \theta_Z)}}{Z'} \right]^* \\ &= \frac{V_R V_S}{Z'} e^{j(\theta_Z - \delta)} - \frac{AV_R^2}{Z'} e^{j(\theta_Z - \theta_A)} \end{aligned} \quad (5.5.2)$$

The real and reactive power delivered to the receiving end are thus

$$P_R = \text{Re}(S_R) = \frac{V_R V_S}{Z'} \cos(\theta_Z - \delta) - \frac{AV_R^2}{Z'} \cos(\theta_Z - \theta_A) \quad (5.5.3)$$

$$Q_R = \text{Im}(S_R) = \frac{V_R V_S}{Z'} \sin(\theta_Z - \delta) - \frac{AV_R^2}{Z'} \sin(\theta_Z - \theta_A) \quad (5.5.4)$$

Note that for a lossless line, $\theta_A = 0^\circ$, $B = Z' = jX'$, $Z' = X'$, $\theta_Z = 90^\circ$, and (5.5.3) reduces to

$$\begin{aligned} P_R &= \frac{V_R V_S}{X'} \cos(90 - \delta) - \frac{AV_R^2}{X'} \cos(90^\circ) \\ &= \frac{V_R V_S}{X'} \sin \delta \end{aligned} \quad (5.5.5)$$

which is the same as (5.4.26).

The theoretical maximum real power delivered (or steady-state stability limit) occurs when $\delta = \theta_Z$ in (5.5.3):

$$P_{R\max} = \frac{V_R V_S}{Z'} - \frac{AV_R^2}{Z'} \cos(\theta_Z - \theta_A) \quad (5.5.6)$$

The second term in (5.5.6), and the fact that Z' is larger than X' , reduce $P_{R\max}$ to a value somewhat less than that given by (5.4.27) for a lossless line.

EXAMPLE 5.5 Theoretical maximum power delivered: long line

Determine the theoretical maximum power, in MW and in per-unit of SIL, that the line in Example 5.2 can deliver. Assume $V_S = V_R = 765$ kV.

SOLUTION From Example 5.2,

$$A = 0.9313 \text{ per unit}; \quad \theta_A = 0.209^\circ$$

$$B = Z' = 97.0 \ \Omega; \quad \theta_Z = 87.2^\circ$$

$$Z_c = 266.1 \ \Omega$$

From (5.5.6) with $V_S = V_R = 765$ kV,

$$\begin{aligned} P_{R\max} &= \frac{(765)^2}{97} - \frac{(0.9313)(765)^2}{97} \cos(87.2^\circ - 0.209^\circ) \\ &= 6033 - 295 = 5738 \text{ MW} \end{aligned}$$

From (5.4.20),

$$\text{SIL} = \frac{(765)^2}{266.1} = 2199 \text{ MW}$$

Thus

$$P_{R\max} = \frac{5738}{2199} = 2.61 \text{ per unit}$$

This value is about 4% less than that found in Example 5.4, where losses were neglected. ■

5.6

LINE LOADABILITY

In practice, power lines are not operated to deliver their theoretical maximum power, which is based on rated terminal voltages and an angular displacement $\delta = 90^\circ$ across the line. Figure 5.12 shows a practical line loadability curve plotted below the theoretical steady-state stability limit. This curve is based on the voltage-drop limit $V_R/V_S \geq 0.95$ and on a maximum angular displacement of 30 to 35° across the line (or about 45° across the line and equivalent system reactances), in order to maintain stability during transient disturbances [1, 3]. The curve is valid for typical overhead 60-Hz lines with no compensation. Note that for short lines less than 80 km long, loadability is limited by the thermal rating of the conductors or by terminal equipment ratings, not by voltage drop or stability considerations. In Section 5.7, we investigate series and shunt compensation techniques to increase the loadability of longer lines toward their thermal limit.

EXAMPLE 5.6 Practical line loadability and percent voltage regulation: long line

The 300-km uncompensated line in Example 5.2 has four 1,272,000-cmil (644.5-mm^2) 54/3 ACSR conductors per bundle. The sending-end voltage is held constant at 1.0 per-unit of rated line voltage. Determine the following:

- The practical line loadability. (Assume an approximate receiving-end voltage $V_R = 0.95$ per unit and $\delta = 35^\circ$ maximum angle across the line.)
- The full-load current at 0.986 p.f. leading based on the above practical line loadability
- The exact receiving-end voltage for the full-load current found in part (b)
- Percent voltage regulation for the above full-load current
- Thermal limit of the line, based on the approximate current-carrying capacity given in Table A.4

SOLUTION

- From (5.5.3), with $V_S = 765$, $V_R = 0.95 \times 765$ kV, and $\delta = 35^\circ$, using the values of Z' , θ_Z , A , and θ_A from Example 5.5,

$$\begin{aligned} P_R &= \frac{(765)(0.95 \times 765)}{97.0} \cos(87.2^\circ - 35^\circ) \\ &\quad - \frac{(0.9313)(0.95 \times 765)^2}{97.0} \cos(87.2^\circ - 0.209^\circ) \\ &= 3513 - 266 = 3247 \text{ MW} \end{aligned}$$

$P_R = 3247$ MW is the practical line loadability, provided the thermal and voltage-drop limits are not exceeded. Alternatively, from Figure 5.12 for a 300-km line, the practical line loadability is $(1.49)\text{SIL} = (1.49)(2199) = 3277$ MW, about the same as the above result.

- b. For the above loading at 0.986 p.f. leading and at 0.95×765 kV, the full-load receiving-end current is

$$I_{\text{RFL}} = \frac{P}{\sqrt{3}V_R(\text{p.f.})} = \frac{3247}{(\sqrt{3})(0.95 \times 765)(0.986)} = 2.616 \text{ kA}$$

- c. From (5.1.1) with $I_{\text{RFL}} = 2.616/\cos^{-1} 0.986 = 2.616/9.599^\circ$ kA, using the A and B parameters from Example 5.2,

$$V_S = AV_{\text{RFL}} + BI_{\text{RFL}}$$

$$\frac{765}{\sqrt{3}} \angle \delta = (0.9313 \angle 0.209^\circ)(V_{\text{RFL}} \angle 0^\circ) + (97.0 \angle 87.2^\circ)(2.616 \angle 9.599^\circ)$$

$$441.7 \angle \delta = (0.9313V_{\text{RFL}} - 30.04) + j(0.0034V_{\text{RFL}} + 251.97)$$

Taking the squared magnitude of the above equation,

$$(441.7)^2 = 0.8673V_{\text{RFL}}^2 - 54.24V_{\text{RFL}} + 64,391$$

Solving,

$$\begin{aligned} V_{\text{RFL}} &= 420.7 \text{ kV}_{\text{LN}} \\ &= 420.7\sqrt{3} = 728.7 \text{ kV}_{\text{LL}} = 0.953 \text{ per unit} \end{aligned}$$

- d. From (5.1.19), the receiving-end no-load voltage is

$$V_{\text{RNL}} = \frac{V_S}{A} = \frac{765}{0.9313} = 821.4 \text{ kV}_{\text{LL}}$$

And from (5.1.18),

$$\text{percent VR} = \frac{821.4 - 728.7}{728.7} \times 100 = 12.72\%$$

- e. From Table A.4, the approximate current-carrying capacity of four 1,272,000-cmil (644.5-mm^2) 54/3 ACSR conductors is $4 \times 1.2 = 4.8$ kA.

Since the voltages $V_S = 1.0$ and $V_{\text{RFL}} = 0.953$ per unit satisfy the voltage-drop limit $V_R/V_S \geq 0.95$, the factor that limits line loadability is steady-state stability for this 300-km uncompensated line. The full-load current of 2.616 kA corresponding to loadability is also well below the thermal limit of 4.8 kA. The 12.7% voltage regulation is too high because the no-load voltage is too high. Compensation techniques to reduce no-load voltages are discussed in Section 5.7. ■

EXAMPLE 5.7 Selection of transmission line voltage and number of lines for power transfer

From a hydroelectric power plant 9000 MW are to be transmitted to a load center located 500 km from the plant. Based on practical line loadability criteria, determine the number of three-phase, 60-Hz lines required to transmit this power, with one line out of service, for the following cases: (a) 345-kV lines with $Z_c = 297 \Omega$; (b) 500-kV lines with $Z_c = 277 \Omega$; (c) 765-kV lines with $Z_c = 266 \Omega$. Assume $V_S = 1.0$ per unit, $V_R = 0.95$ per unit, and $\delta = 35^\circ$. Also assume that the lines are uncompensated and widely separated such that there is negligible mutual coupling between them.

SOLUTION

a. For 345-kV lines, (5.4.21) yields

$$\text{SIL} = \frac{(345)^2}{297} = 401 \text{ MW}$$

Neglecting losses, from (5.4.29), with $l = 500$ km and $\delta = 35^\circ$,

$$P = \frac{(1.0)(0.95)(401) \sin(35^\circ)}{\sin\left(\frac{2\pi \times 500}{5000}\right)} = (401)(0.927) = 372 \text{ MW/line}$$

Alternatively, the practical line loadability curve in Figure 5.12 can be used to obtain $P = (0.93)\text{SIL}$ for typical 500-km overhead 60-Hz uncompensated lines.

In order to transmit 9000 MW with one line out of service,

$$\#345\text{-kV lines} = \frac{9000 \text{ MW}}{372 \text{ MW/line}} + 1 = 24.2 + 1 \approx 26$$

b. For 500-kV lines,

$$\text{SIL} = \frac{(500)^2}{277} = 903 \text{ MW}$$

$$P = (903)(0.927) = 837 \text{ MW/line}$$

$$\#500\text{-kV lines} = \frac{9000}{837} + 1 = 10.8 + 1 \approx 12$$

c. For 765-kV lines,

$$\text{SIL} = \frac{(765)^2}{266} = 2200 \text{ MW}$$

$$P = (2200)(0.927) = 2039 \text{ MW/line}$$

$$\#765\text{-kV lines} = \frac{9000}{2039} + 1 = 4.4 + 1 \approx 6$$

Increasing the line voltage from 345 to 765 kV, a factor of 2.2, reduces the required number of lines from 26 to 6, a factor of 4.3. ■

EXAMPLE 5.8 Effect of intermediate substations on number of lines required for power transfer

Can five instead of six 765-kV lines transmit the required power in Example 5.7 if there are two intermediate substations that divide each line into three 167-km line sections, and if only one line section is out of service?

SOLUTION The lines are shown in Figure 5.14. For simplicity, we neglect line losses. The equivalent π circuit of one 500-km, 765-kV line has a series reactance, from (5.4.10) and (5.4.15),

$$X' = (266) \sin\left(\frac{2\pi \times 500}{5000}\right) = 156.35 \quad \Omega$$

Combining series/parallel reactances in Figure 5.14, the equivalent reactance of five lines with one line section out of service is

$$X_{\text{eq}} = \frac{1}{5} \left(\frac{2}{3} X' \right) + \frac{1}{4} \left(\frac{X'}{3} \right) = 0.2167X' = 33.88 \quad \Omega$$

Then, from (5.4.26) with $\delta = 35^\circ$,

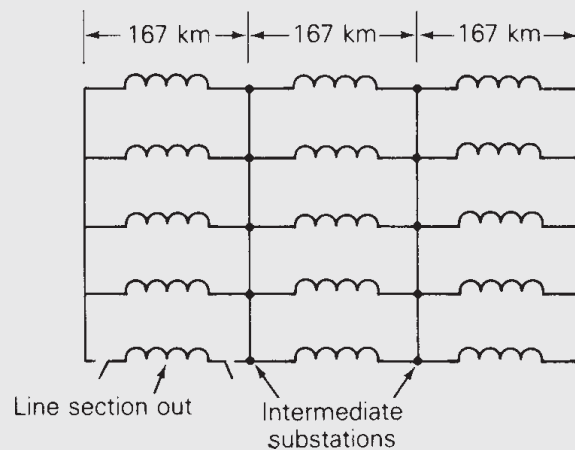
$$P = \frac{(765)(765 \times 0.95) \sin(35^\circ)}{33.88} = 9412 \quad \text{MW}$$

Inclusion of line losses would reduce the above value by 3 or 4% to about 9100 MW. Therefore, the answer is yes. Five 765-kV, 500-km uncompensated lines with two intermediate substations and with one line section out of service will transmit 9000 MW. Intermediate substations are often economical if their costs do not outweigh the reduction in line costs.

This example is modeled in PowerWorld Simulator case Example 5_8 (see Figure 5.15). Each line segment is represented with the lossless line model from Example 5.4 with the π circuit parameters modified to exactly match those for a 167 km distributed line. The pie charts on each line segment show the percentage loading of the line, assuming a rating of 3500 MVA. The solid red squares on the lines represent closed circuit breakers,

FIGURE 5.14

Transmission-line configuration for Example 5.8



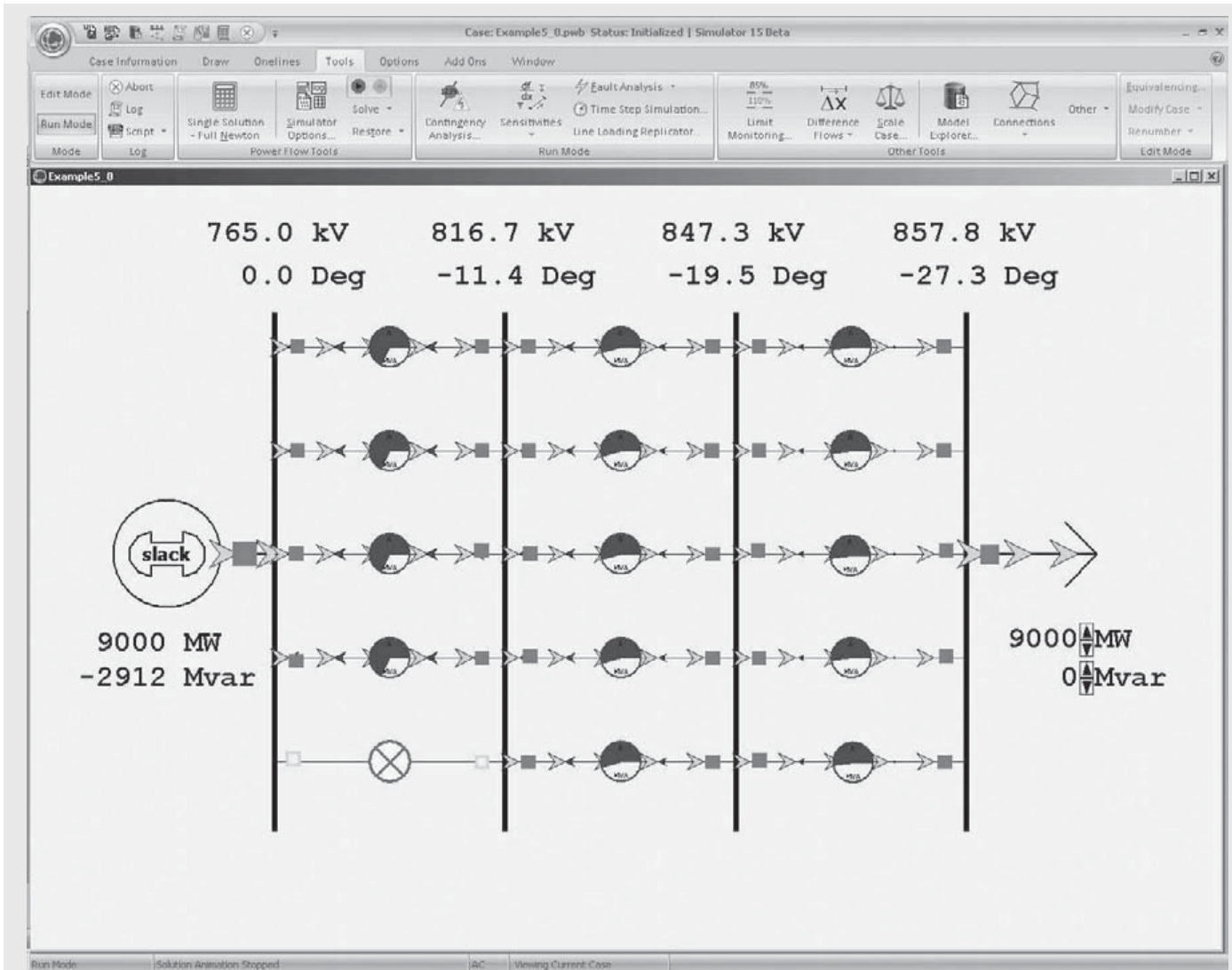


FIGURE 5.15 Screen for Example 5.8

and the green squares correspond to open circuit breakers. Clicking on a circuit breaker toggles its status. The simulation results differ slightly from the simplified analysis done earlier in the example because the simulation includes the charging capacitance of the transmission lines. With all line segments in-service, use the load's arrow to verify that the SIL for this system is 11,000 MW, five times that of the single circuit line in Example 5.4. ■

5.7

REACTIVE COMPENSATION TECHNIQUES

Inductors and capacitors are used on medium-length and long transmission lines to increase line loadability and to maintain voltages near rated values.

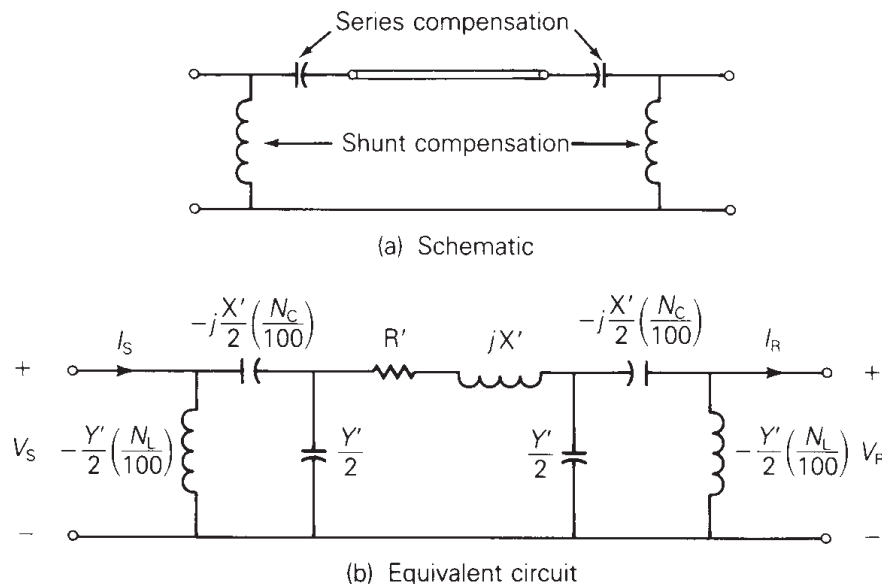
Shunt reactors (inductors) are commonly installed at selected points along EHV lines from each phase to neutral. The inductors absorb reactive power and reduce overvoltages during light load conditions. They also reduce transient overvoltages due to switching and lightning surges. However, shunt reactors can reduce line loadability if they are not removed under full-load conditions.

In addition to shunt reactors, shunt capacitors are sometimes used to deliver reactive power and increase transmission voltages during heavy load conditions. Another type of shunt compensation includes thyristor-switched reactors in parallel with capacitors. These devices, called *static var compensators*, can absorb reactive power during light loads and deliver reactive power during heavy loads. Through automatic control of the thyristor switches, voltage fluctuations are minimized and line loadability is increased. Synchronous condensers (synchronous motors with no mechanical load) can also control their reactive power output, although more slowly than static var compensators.

Series capacitors are sometimes used on long lines to increase line loadability. Capacitor banks are installed in series with each phase conductor at selected points along a line. Their effect is to reduce the net series impedance of the line in series with the capacitor banks, thereby reducing line-voltage drops and increasing the steady-state stability limit. A disadvantage of series capacitor banks is that automatic protection devices must be installed to bypass high currents during faults and to reinsert the capacitor banks after fault clearing. Also, the addition of series capacitors can excite low-frequency oscillations, a phenomenon called *subsynchronous resonance*, which may damage turbine-generator shafts. Studies have shown, however, that series capacitive compensation can increase the loadability of long lines at only a fraction of the cost of new transmission [1].

Figure 5.16 shows a schematic and an equivalent circuit for a compensated line section, where N_C is the amount of series capacitive compensation

FIGURE 5.16
Compensated transmission-line section



expressed in percent of the positive-sequence line impedance and N_L is the amount of shunt reactive compensation in percent of the positive-sequence line admittance. It is assumed in Figure 5.16 that half of the compensation is installed at each end of the line section. The following two examples illustrate the effect of compensation.

EXAMPLE 5.9 Shunt reactive compensation to improve transmission-line voltage regulation

Identical shunt reactors (inductors) are connected from each phase conductor to neutral at both ends of the 300-km line in Example 5.2 during light load conditions, providing 75% compensation. The reactors are removed during heavy load conditions. Full load is 1.90 kA at unity p.f. and at 730 kV. Assuming that the sending-end voltage is constant, determine the following:

- Percent voltage regulation of the uncompensated line
- The equivalent shunt admittance and series impedance of the compensated line
- Percent voltage regulation of the compensated line

SOLUTION

- a. From (5.1.1) with $I_{RFL} = 1.9\angle 0^\circ$ kA, using the A and B parameters from Example 5.2,

$$\begin{aligned} V_S &= AV_{RFL} + BI_{RFL} \\ &= (0.9313\angle 0.209^\circ) \left(\frac{730}{\sqrt{3}} \angle 0^\circ \right) + (97.0\angle 87.2^\circ)(1.9\angle 0^\circ) \\ &= 392.5\angle 0.209^\circ + 184.3\angle 87.2^\circ \\ &= 401.5 + j185.5 \\ &= 442.3\angle 24.8^\circ \text{ kV}_{LN} \end{aligned}$$

$$V_S = 442.3\sqrt{3} = 766.0 \text{ kV}_{LL}$$

The no-load receiving-end voltage is, from (5.1.19),

$$V_{RNL} = \frac{766.0}{0.9313} = 822.6 \text{ kV}_{LL}$$

and the percent voltage regulation for the uncompensated line is, from (5.1.18),

$$\text{percent VR} = \frac{822.6 - 730}{730} \times 100 = 12.68\%$$

- b. From Example 5.3, the shunt admittance of the equivalent π circuit without compensation is

$$\begin{aligned}
 Y' &= 2(3.7 \times 10^{-7} + j7.094 \times 10^{-4}) \\
 &= 7.4 \times 10^{-7} + j14.188 \times 10^{-4} \text{ S}
 \end{aligned}$$

With 75% shunt compensation, the equivalent shunt admittance is

$$\begin{aligned}
 Y_{\text{eq}} &= 7.4 \times 10^{-7} + j14.188 \times 10^{-4} \left(1 - \frac{75}{100}\right) \\
 &= 3.547 \times 10^{-4} / \underline{89.88^\circ} \text{ S}
 \end{aligned}$$

Since there is no series compensation, the equivalent series impedance is the same as without compensation:

$$Z_{\text{eq}} = Z' = 97.0 / \underline{87.2^\circ} \ \Omega$$

c. The equivalent A parameter for the compensated line is

$$\begin{aligned}
 A_{\text{eq}} &= 1 + \frac{Y_{\text{eq}} Z_{\text{eq}}}{2} \\
 &= 1 + \frac{(3.547 \times 10^{-4} / \underline{89.88^\circ})(97.0 / \underline{87.2^\circ})}{2} \\
 &= 1 + 0.0172 / \underline{177.1^\circ} \\
 &= 0.9828 / \underline{0.05^\circ} \text{ per unit}
 \end{aligned}$$

Then, from (5.1.19),

$$V_{\text{RNL}} = \frac{766}{0.9828} = 779.4 \text{ kV}_{\text{LL}}$$

Since the shunt reactors are removed during heavy load conditions, $V_{\text{RFL}} = 730 \text{ kV}$ is the same as without compensation. Therefore

$$\text{percent VR} = \frac{779.4 - 730}{730} \times 100 = 6.77\%$$

The use of shunt reactors at light loads improves the voltage regulation from 12.68% to 6.77% for this line. ■

EXAMPLE 5.10 Series capacitive compensation to increase transmission-line loadability

Identical series capacitors are installed in each phase at both ends of the line in Example 5.2, providing 30% compensation. Determine the theoretical maximum power that this compensated line can deliver and compare with that of the uncompensated line. Assume $V_S = V_R = 765 \text{ kV}$.

SOLUTION From Example 5.3, the equivalent series reactance without compensation is

$$X' = 97.0 \sin 87.2^\circ = 96.88 \ \Omega$$

Based on 30% series compensation, half at each end of the line, the impedance of each series capacitor is

$$Z_{\text{cap}} = -jX_{\text{cap}} = -j\left(\frac{1}{2}\right)(0.30)(96.88) = -j14.53 \quad \Omega$$

From Figure 5.4, the $ABCD$ matrix of this series impedance is

$$\left[\begin{array}{c|c} 1 & -j14.53 \\ \hline 0 & 1 \end{array} \right]$$

As also shown in Figure 5.4, the equivalent $ABCD$ matrix of networks in series is obtained by multiplying the $ABCD$ matrices of the individual networks. For this example there are three networks: the series capacitors at the sending end, the line, and the series capacitors at the receiving end. Therefore the equivalent $ABCD$ matrix of the compensated line is, using the $ABCD$ parameters, from Example 5.2,

$$\left[\begin{array}{c|c} 1 & -j14.53 \\ \hline 0 & 1 \end{array} \right] \left[\begin{array}{c|c} 0.9313/\underline{0.209^\circ} & 97.0/\underline{87.2^\circ} \\ \hline 1.37 \times 10^{-3}/\underline{90.06^\circ} & 0.9313/\underline{0.209^\circ} \end{array} \right] \left[\begin{array}{c|c} 1 & -j14.53 \\ \hline 0 & 1 \end{array} \right]$$

After performing these matrix multiplications, we obtain

$$\left[\begin{array}{c|c} A_{\text{eq}} & B_{\text{eq}} \\ \hline C_{\text{eq}} & D_{\text{eq}} \end{array} \right] = \left[\begin{array}{c|c} 0.9512/\underline{0.205^\circ} & 69.70/\underline{86.02^\circ} \\ \hline 1.37 \times 10^{-3}/\underline{90.06^\circ} & 0.9512/\underline{0.205^\circ} \end{array} \right]$$

Therefore

$$A_{\text{eq}} = 0.9512 \quad \text{per unit} \quad \theta_{A_{\text{eq}}} = 0.205^\circ$$

$$B_{\text{eq}} = Z'_{\text{eq}} = 69.70 \quad \Omega \quad \theta_{Z_{\text{eq}}} = 86.02^\circ$$

From (5.5.6) with $V_S = V_R = 765$ kV,

$$\begin{aligned} P_{\text{Rmax}} &= \frac{(765)^2}{69.70} - \frac{(0.9512)(765)^2}{69.70} \cos(86.02^\circ - 0.205^\circ) \\ &= 8396 - 583 = 7813 \quad \text{MW} \end{aligned}$$

which is 36.2% larger than the value of 5738 MW found in Example 5.5 without compensation. We note that the practical line loadability of this series compensated line is also about 35% larger than the value of 3247 MW found in Example 5.6 without compensation.

This example is modeled in PowerWorld Simulator case Example 5_10 (see Figure 5.17). When opened, both of the series capacitors are bypassed (i.e., they are modeled as short circuits) meaning this case is initially identical to the Example 5.4 case. Click on the blue “Bypassed” field to place each of the series capacitors into the circuit. This decreases the angle across the line, resulting in more net power transfer.

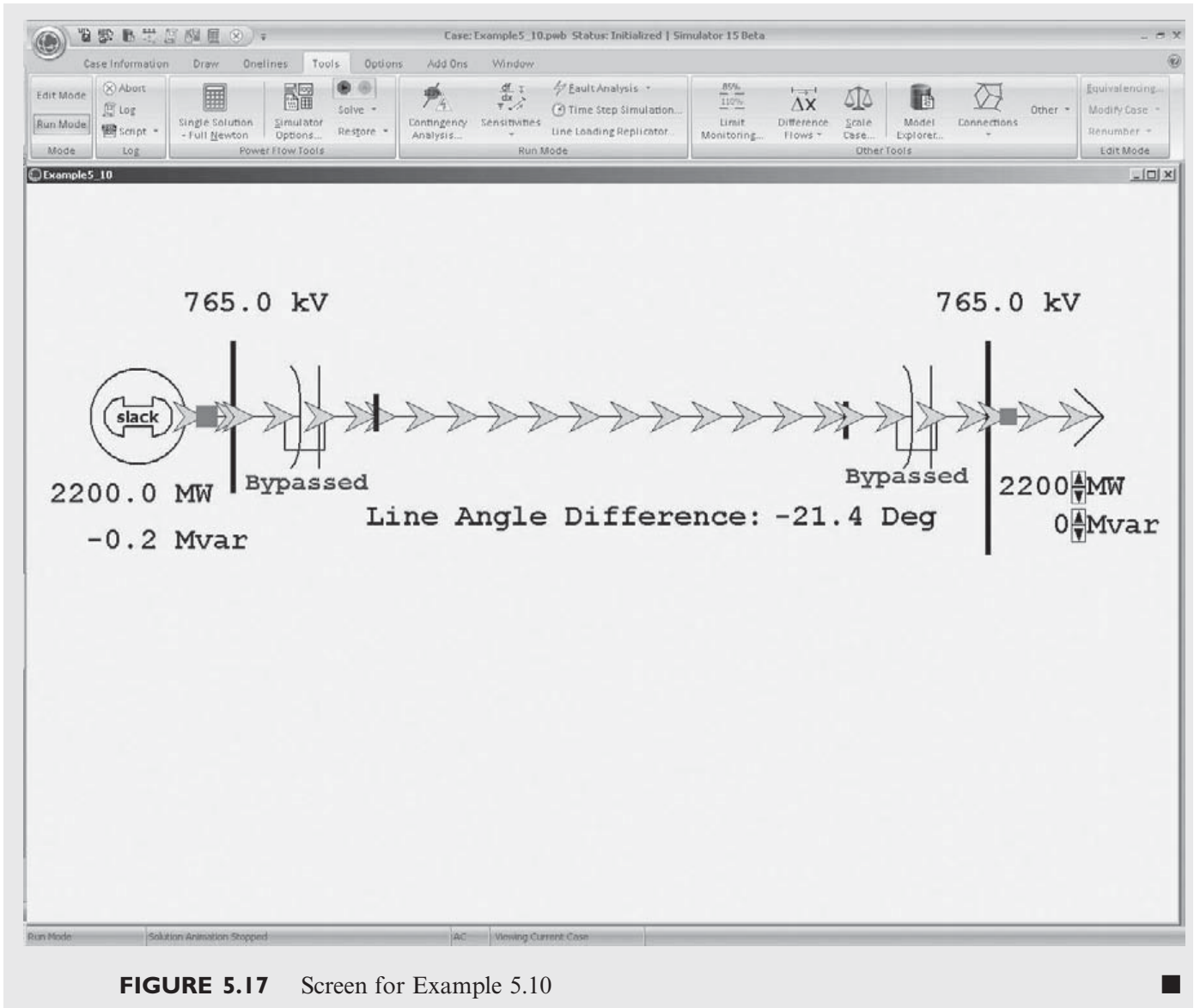


FIGURE 5.17 Screen for Example 5.10

MULTIPLE CHOICE QUESTIONS

SECTION 5.1

- 5.1 Representing a transmission line by the two-port network, in terms of $ABCD$ parameters, (a) express V_S , the sending-end voltage, in terms of V_R , the receiving-end voltage, and I_R , the receiving-end current, and (b) express I_S , the sending-end current, in terms of V_R and I_R .
 (a) $V_S =$ _____ (b) $I_S =$ _____
- 5.2 As applied to linear, passive, bilateral two-port networks, the $ABCD$ parameters satisfy $AD - BC = 1$.
 (a) True (b) False
- 5.3 Express the no-load receiving-end voltage V_{RNL} in terms of the sending-end voltage, V_S , and the $ABCD$ parameters.
 $V_{RNL} =$ _____

- 5.4** The $ABCD$ parameters, which are in general complex numbers, have the units of _____, _____, _____, _____, respectively. Fill in the Blanks.
- 5.5** The loadability of short transmission lines (less than 80 km, represented by including only series resistance and reactance) is determined by _____; that of medium lines (less than 250 km, represented by nominal π circuit) is determined by _____; and that of long lines (more than 250 km, represented by equivalent π circuit) is determined by _____. Fill in the Blanks.
- 5.6** Can the voltage regulation, which is proportional to $(V_{RNL} - V_{RFL})$, be negative?
 (a) Yes (b) No

SECTION 5.2

- 5.7** The propagation constant, which is a complex quantity in general, has the units of _____, and the characteristic impedance has the units of _____.
- 5.8** Express hyperbolic functions $\cosh \sqrt{x}$ and $\sinh \sqrt{x}$ in terms of exponential functions.
- 5.9** e^{γ} , where $\gamma = \alpha + j\beta$, can be expressed as $e^{\alpha l} / \beta l$, in which αl is dimensionless and βl is in radians (also dimensionless).
 (a) True (b) False

SECTION 5.3

- 5.10** The equivalent π circuit is identical in structure to the nominal π circuit.
 (a) True (b) False
- 5.11** The correction factors $F_1 = \sinh(\gamma l) / \gamma l$ and $F_2 = \tanh(\gamma l / 2) / (\gamma l / 2)$, which are complex numbers, have the units of _____. Fill in the Blank.

SECTION 5.4

- 5.12** For a lossless line, the surge impedance is purely resistive and the propagation constant is pure imaginary.
 (a) True (b) False
- 5.13** For equivalent π circuits of lossless lines, the A and D parameters are pure _____. whereas B and C parameters are pure _____. Fill in the Blanks.
- 5.14** In equivalent π circuits of lossless lines, Z' is pure _____, and Y' is pure _____. Fill in the Blanks.
- 5.15** Typical power-line lengths are only a small fraction of the 60-Hz wavelength.
 (a) True (b) False
- 5.16** The velocity of propagation of voltage and current waves along a lossless overhead line is the same as speed of light.
 (a) True (b) False
- 5.17** Surge Impedance Loading (SIL) is the power delivered by a lossless line to a load resistance equal to _____. Fill in the Blank.
- 5.18** For a lossless line, at SIL, the voltage profile is _____, and the real power delivered, in terms of rated line voltage V and surge impedance Z_C , is given by _____. Fill in the Blanks.

- 5.19** The maximum power that a lossless line can deliver, in terms of the voltage magnitudes V_S and V_R (in volts) at the ends of the line held constant, and the series reactance X' of the corresponding equivalent π circuit, is given by _____, in Watts. Fill in the Blank.

SECTION 5.5

- 5.20** The maximum power flow for a lossy line will be somewhat less than that for a lossless line.
 (a) True (b) False

SECTION 5.6

- 5.21** For short lines less than 80 km long, loadability is limited by the thermal rating of the conductors or by terminal equipment ratings, not by voltage drop or stability considerations.
 (a) True (b) False
- 5.22** Increasing the transmission line voltage reduces the required number of lines for the same power transfer.
 (a) True (b) False
- 5.23** Intermediate substations are often economical from the viewpoint of the number of lines required for power transfer, if their costs do not outweigh the reduction in line costs.
 (a) True (b) False

SECTION 5.7

- 5.24** Shunt reactive compensation improves transmission-line _____, whereas series capacitive compensation increases transmission-line _____. Fill in the Blanks.
- 5.25** Static-var-compensators can absorb reactive power during light loads, and deliver reactive power during heavy loads.
 (a) True (b) False

PROBLEMS

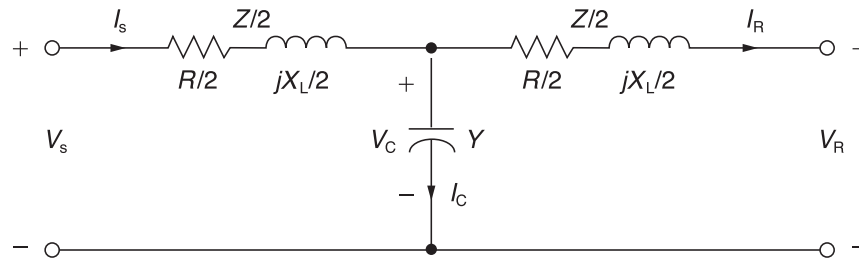
SECTION 5.1

- 5.1** A 25-km, 34.5-kV, 60-Hz three-phase line has a positive-sequence series impedance $z = 0.19 + j0.34 \Omega/\text{km}$. The load at the receiving end absorbs 10 MVA at 33 kV. Assuming a short line, calculate: (a) the $ABCD$ parameters, (b) the sending-end voltage for a load power factor of 0.9 lagging, (c) the sending-end voltage for a load power factor of 0.9 leading.
- 5.2** A 200-km, 230-kV, 60-Hz three-phase line has a positive-sequence series impedance $z = 0.08 + j0.48 \Omega/\text{km}$ and a positive-sequence shunt admittance $y = j3.33 \times 10^{-6} \text{ S}/\text{km}$. At full load, the line delivers 250 MW at 0.99 p.f. lagging and at 220 kV. Using the nominal π circuit, calculate: (a) the $ABCD$ parameters, (b) the sending-end voltage and current, and (c) the percent voltage regulation.

- 5.3** Rework Problem 5.2 in per-unit using 100-MVA (three-phase) and 230-kV (line-to-line) base values. Calculate: (a) the per-unit $ABCD$ parameters, (b) the per-unit sending-end voltage and current, and (c) the percent voltage regulation.
- 5.4** Derive the $ABCD$ parameters for the two networks in series, as shown in Figure 5.4.
- 5.5** Derive the $ABCD$ parameters for the T circuit shown in Figure 5.4.
- 5.6** (a) Consider a medium-length transmission line represented by a nominal π circuit shown in Figure 5.3 of the text. Draw a phasor diagram for lagging power-factor condition at the load (receiving end).
- (b) Now consider a nominal T-circuit of the medium-length transmission line shown in Figure 5.18.
- (i) Draw the corresponding phasor diagram for lagging power-factor load condition
- (ii) Determine the $ABCD$ parameters in terms of Y and Z , for the nominal T-circuit and for the nominal π -circuit of part (a).

FIGURE 5.18

Nominal T-circuit for Problem 5.6



- 5.7** The per-phase impedance of a short three—phase transmission line is $0.5/\underline{53.15^\circ}\Omega$. The three-phase load at the receiving end is 900 kW at 0.8 p.f. lagging. If the line-to-line sending-end voltage is 3.3 kV, determine (a) the receiving-end line-to-line voltage in kV, and (b) the line current. Draw the phasor diagram with the line current I , as reference.
- 5.8** Reconsider Problem 5.7 and find the following: (a) sending-end power factor, (b) sending-end three-phase power, and (c) the three-phase line loss.
- 5.9** The 100-km, 230-kV, 60-Hz three-phase line in Problems 4.18 and 4.39 delivers 300 MVA at 218 kV to the receiving end at full load. Using the nominal π circuit, calculate the: $ABCD$ parameters, sending-end voltage, and percent voltage regulation when the receiving-end power factor is (a) 0.9 lagging, (b) unity, and (c) 0.9 leading. Assume a 50°C conductor temperature to determine the resistance of this line.
- 5.10** The 500-kV, 60-Hz three-phase line in Problems 4.20 and 4.41 has a 180-km length and delivers 1600 MW at 475 kV and at 0.95 power factor leading to the receiving end at full load. Using the nominal π circuit, calculate the: (a) $ABCD$ parameters, (b) sending-end voltage and current, (c) sending-end power and power factor, (d) full-load line losses and efficiency, and (e) percent voltage regulation. Assume a 50°C conductor temperature to determine the resistance of this line.
- 5.11** A 40-km, 220-kV, 60-Hz three-phase overhead transmission line has a per-phase resistance of $0.15 \Omega/\text{km}$, a per-phase inductance of $1.3263 \text{ mH}/\text{km}$, and negligible shunt capacitance. Using the short line model, find the sending-end voltage, voltage regulation, sending-end power, and transmission line efficiency when the line is supplying a three-phase load of: (a) 381 MVA at 0.8 power factor lagging and at 220 kV, (b) 381 MVA at 0.8 power factor leading and at 220 kV.

- 5.12** A 60-Hz, 100-km, three-phase overhead transmission line, constructed of ACSR conductors, has a series impedance of $(0.1826 + j0.784) \Omega/\text{km}$ per phase and a shunt capacitive reactance-to-neutral of $185.5 \times 10^3 / -90^\circ \Omega\text{-km}$ per phase. Using the nominal π circuit for a medium-length transmission line, (a) determine the total series impedance and shunt admittance of the line. (b) Compute the voltage, the current, and the real and reactive power at the sending end if the load at the receiving end draws 200 MVA at unity power factor and at a line-to-line voltage of 230 kV. (c) Find the percent voltage regulation of the line.

SECTION 5.2

- 5.13** Evaluate $\cosh(\gamma l)$ and $\tanh(\gamma l/2)$ for $\gamma l = 0.40 / 85^\circ$ per unit.
- 5.14** A 400-km, 500-kV, 60-Hz uncompensated three-phase line has a positive-sequence series impedance $z = 0.03 + j0.35 \Omega/\text{km}$ and a positive-sequence shunt admittance $y = j4.4 \times 10^{-6} \text{ S/km}$. Calculate: (a) Z_c , (b) (γl) , and (c) the exact $ABCD$ parameters for this line.
- 5.15** At full load the line in Problem 5.14 delivers 1000 MW at unity power factor and at 475 kV. Calculate: (a) the sending-end voltage, (b) the sending-end current, (c) the sending-end power factor, (d) the full-load line losses, and (e) the percent voltage regulation.
- 5.16** The 500-kV, 60-Hz three-phase line in Problems 4.20 and 4.41 has a 300-km length. Calculate: (a) Z_c , (b) (γl) , and (c) the exact $ABCD$ parameters for this line. Assume a 50°C conductor temperature.
- 5.17** At full load, the line in Problem 5.16 delivers 1500 MVA at 480 kV to the receiving-end load. Calculate the sending-end voltage and percent voltage regulation when the receiving-end power factor is (a) 0.9 lagging, (b) unity, and (c) 0.9 leading.
- 5.18** A 60-Hz, 230-km, three-phase overhead transmission line has a series impedance $z = 0.8431 / 79.04^\circ \Omega/\text{km}$ and a shunt admittance $y = 5.105 \times 10^{-6} / 90^\circ \text{ S/km}$. The load at the receiving end is 125 MW at unity power factor and at 215 kV. Determine the voltage, current, real and reactive power at the sending end and the percent voltage regulation of the line. Also find the wavelength and velocity of propagation of the line.
- 5.19** Using per-unit calculations, rework Problem 5.18 to determine the sending-end voltage and current.
- 5.20** (a) The series expansions of the hyperbolic functions are given by

$$\cosh \theta = 1 + \frac{\theta^2}{2} + \frac{\theta^4}{24} + \frac{\theta^6}{720} + \dots$$

$$\sinh \theta = \theta + \frac{\theta^3}{6} + \frac{\theta^5}{120} + \frac{\theta^7}{5040} + \dots$$

For the $ABCD$ parameters of a long transmission line represented by an equivalent π circuit, apply the above expansion and consider only the first two terms, and express the result in terms of Y and Z .

- (b) For the nominal π and equivalent π circuits shown in Figures 5.3 and 5.7 of the text, show that

$$\frac{A-1}{B} = \frac{Y}{2} \quad \text{and} \quad \frac{A-1}{B} = \frac{Y'}{2}$$

hold good, respectively.

5.21 Starting with (5.1.1) of the text, show that

$$A = \frac{V_S I_S + V_R I_R}{V_R I_S + V_S I_R} \quad \text{and} \quad B = \frac{V_S^2 - V_R^2}{V_R I_S + V_S I_R}$$

5.22 Consider the A parameter of the long line given by $\cosh \theta$, where $\theta = \sqrt{ZY}$. With $x = e^{-\theta} = x_1 + jx_2$, and $A = A_1 + jA_2$, show that x_1 and x_2 satisfy the following:

$$x_1^2 - x_2^2 - 2(A_1 x_1 - A_2 x_2) + 1 = 0$$

$$\text{and} \quad x_1 x_2 - (A_2 x_1 + A_1 x_2) = 0.$$

SECTION 5.3

5.23 Determine the equivalent π circuit for the line in Problem 5.14 and compare it with the nominal π circuit.

5.24 Determine the equivalent π circuit for the line in Problem 5.16. Compare the equivalent π circuit with the nominal π circuit.

5.25 Let the transmission line of Problem 5.12 be extended to cover a distance of 200 km. Assume conditions at the load to be the same as in Problem 5.12. Determine the: (a) sending-end voltage, (b) sending-end current, (c) sending-end real and reactive powers, and (d) percent voltage regulation.

SECTION 5.4

5.26 A 300-km, 500-kV, 60-Hz three-phase uncompensated line has a positive-sequence series reactance $x = 0.34 \Omega/\text{km}$ and a positive-sequence shunt admittance $y = j4.5 \times 10^{-6} \text{ S/km}$. Neglecting losses, calculate: (a) Z_c , (b) (γl) , (c) the $ABCD$ parameters, (d) the wavelength λ of the line, in kilometers, and (e) the surge impedance loading in MW.

5.27 Determine the equivalent π circuit for the line in Problem 5.26.

5.28 Rated line voltage is applied to the sending end of the line in Problem 5.26. Calculate the receiving-end voltage when the receiving end is terminated by (a) an open circuit, (b) the surge impedance of the line, and (c) one-half of the surge impedance. (d) Also calculate the theoretical maximum real power that the line can deliver when rated voltage is applied to both ends of the line.

5.29 Rework Problems 5.9 and 5.16 neglecting the conductor resistance. Compare the results with and without losses.

5.30 From (4.6.22) and (4.10.4), the series inductance and shunt capacitance of a three-phase overhead line are

$$L_a = 2 \times 10^{-7} \ln(D_{\text{eq}}/D_{\text{SL}}) = \frac{\mu_0}{2\pi} \ln(D_{\text{eq}}/D_{\text{SL}}) \quad \text{H/m}$$

$$C_{\text{an}} = \frac{2\pi\epsilon_0}{\ln(D_{\text{eq}}/D_{\text{SC}})} \quad \text{F/m}$$

$$\text{where } \mu_0 = 4\pi \times 10^{-7} \text{ H/m and } \epsilon_0 = \left(\frac{1}{36\pi}\right) \times 10^{-9} \text{ F/m}$$

Using these equations, determine formulas for surge impedance and velocity of propagation of an overhead lossless line. Then determine the surge impedance and velocity of propagation for the three-phase line given in Example 4.5. Assume positive-sequence operation. Neglect line losses as well as the effects of the overhead neutral wires and the earth plane.

- 5.31** A 500-kV, 300-km, 60-Hz three-phase overhead transmission line, assumed to be lossless, has a series inductance of 0.97 mH/km per phase and a shunt capacitance of 0.0115 μ F/km per phase. (a) Determine the phase constant β , the surge impedance Z_C , velocity of propagation v , and the wavelength λ of the line. (b) Determine the voltage, current, real and reactive power at the sending end, and the percent voltage regulation of the line if the receiving-end load is 800 MW at 0.8 power factor lagging and at 500 kV.
- 5.32** The following parameters are based on a preliminary line design: $V_S = 1.0$ per unit, $V_R = 0.9$ per unit, $\lambda = 5000$ km, $Z_C = 320 \Omega$, $\delta = 36.8^\circ$. A three-phase power of 700 MW is to be transmitted to a substation located 315 km from the source of power. (a) Determine a nominal voltage level for the three-phase transmission line, based on the practical line-loadability equation. (b) For the voltage level obtained in (a), determine the theoretical maximum power that can be transferred by the line.
- 5.33** Consider a long radial line terminated in its characteristic impedance Z_C . Determine the following:
- V_1/I_1 , known as the driving point impedance.
 - $|V_2|/|V_1|$, known as the voltage gain, in terms of $\alpha\ell$.
 - $|I_2|/|I_1|$, known as the current gain, in terms of $\alpha\ell$.
 - The complex power gain, $-S_{21}/S_{12}$, in terms of $\alpha\ell$.
 - The real power efficiency, $(-P_{21}/P_{12}) = \eta$, in terms of $\alpha\ell$.
- [Note: 1 refers to sending end and 2 refers to receiving end. (S_{21}) is the complex power received at 2; S_{12} is sent from 1.]
- 5.34** For the case of a lossless line, how would the results of Problem 5.33 change? In terms of Z_C , which will be a real quantity for this case, express P_{12} in terms $|I_1|$ and $|V_1|$.
- 5.35** For a lossless open-circuited line, express the sending-end voltage, V_1 , in terms of the receiving-end voltage, V_2 , for the three cases of short-line model, medium-length line model, and long-line model. Is it true that the voltage at the open receiving end of a long line is higher than that at the sending end, for small $\beta\ell$.
- 5.36** For a short transmission line of impedance $(R + jX)$ ohms per phase, show that the maximum power that can be transmitted over the line is

$$P_{\max} = \frac{V_R^2}{Z^2} \left(\frac{ZV_S}{V_R} - R \right) \quad \text{where } Z = \sqrt{R^2 + X^2}$$

when the sending-end and receiving-end voltages are fixed, and for the condition

$$Q = \frac{-V_R^2 X}{R^2 + X^2} \quad \text{when } dP/dQ = 0$$

- 5.37** (a) Consider complex power transmission via the three-phase short line for which the per-phase circuit is shown in Figure 5.19. Express S_{12} , the complex power sent by bus 1 (or V_1), and $(-S_{21})$, the complex power received by bus 2 (or V_2), in terms of V_1 , V_2 , Z , $\angle Z$, and $\theta_{12} = \theta_1 - \theta_2$, the power angle.
- (b) For a balanced three-phase transmission line, in per-unit notation, with $Z = 1/\underline{85^\circ}$, $\theta_{12} = 10^\circ$, determine S_{12} and $(-S_{21})$ for

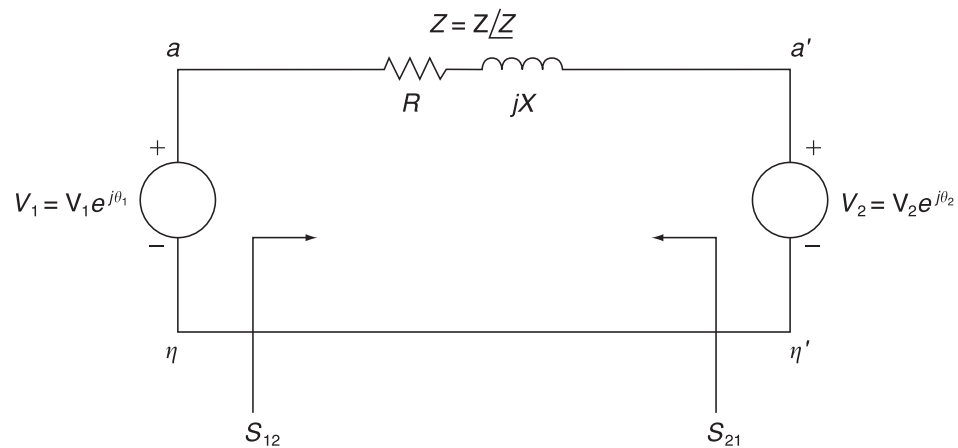
(i) $V_1 = V_2 = 1.0$

(ii) $V_1 = 1.1$ and $V_2 = 0.9$

Comment on the changes of real and reactive powers from (i) to (ii).

FIGURE 5.19

Per-phase circuit for
Problem 5.37



SECTION 5.5

- 5.38** The line in Problem 5.14 has three ACSR 1113-kcmil (564-mm²) conductors per phase. Calculate the theoretical maximum real power that this line can deliver and compare with the thermal limit of the line. Assume $V_S = V_R = 1.0$ per unit and unity power factor at the receiving end.
- 5.39** Repeat Problems 5.14 and 5.38 if the line length is (a) 200 km, (b) 600 km.
- 5.40** For the 500-kV line given in Problem 5.16, (a) calculate the theoretical maximum real power that the line can deliver to the receiving end when rated voltage is applied to both ends. (b) Calculate the receiving-end reactive power and power factor at this theoretical loading.
- 5.41** A 230-kV, 100-km, 60-Hz three-phase overhead transmission line with a rated current of 900 A/phase has a series impedance $z = 0.088 + j0.465 \Omega/\text{km}$ and a shunt admittance $y = j3.524 \mu\text{S}/\text{km}$. (a) Obtain the nominal π equivalent circuit in normal units and in per unit on a base of 100 MVA (three phase) and 230 kV (line-to-line). (b) Determine the three-phase rated MVA of the line. (c) Compute the ABCD parameters. (d) Calculate the SIL.
- 5.42** A three-phase power of 460 MW is to be transmitted to a substation located 500 km from the source of power. With $V_S = 1$ per unit, $V_R = 0.9$ per unit, $\lambda = 5000 \text{ km}$, $Z_C = 500 \Omega$, and $\delta = 36.87^\circ$, determine a nominal voltage level for the lossless transmission line, based on Eq. (5.4.29) of the text. Using this result, find the theoretical three-phase maximum power that can be transferred by the lossless transmission line.
- PW** **5.43** Open PowerWorld Simulator case Example 5_4 and graph the load bus voltage as a function of load real power (assuming unity power factor at the load). What is the maximum amount of real power that can be transferred to the load at unity power factor if we require the load voltage always be greater than 0.9 per unit?

- PW** 5.44 Repeat Problem 5.43, but now vary the load reactive power, assuming the load real power is fixed at 1000 MW.

SECTION 5.6

- 5.45 For the line in Problems 5.14 and 5.38, determine: (a) the practical line loadability in MW, assuming $V_S = 1.0$ per unit, $V_R \approx 0.95$ per unit, and $\delta_{\max} = 35^\circ$; (b) the full-load current at 0.99 p.f. leading, based on the above practical line loadability; (c) the exact receiving-end voltage for the full-load current in (b) above; and (d) the percent voltage regulation. For this line, is loadability determined by the thermal limit, the voltage-drop limit, or steady-state stability?
- 5.46 Repeat Problem 5.45 for the 500-kV line given in Problem 5.10.
- 5.47 Determine the practical line loadability in MW and in per-unit of SIL for the line in Problem 5.14 if the line length is (a) 200 km, (b) 600 km. Assume $V_S = 1.0$ per unit, $V_R = 0.95$ per unit, $\delta_{\max} = 35^\circ$, and 0.99 leading power factor at the receiving end.
- 5.48 It is desired to transmit 2000 MW from a power plant to a load center located 300 km from the plant. Determine the number of 60-Hz three-phase, uncompensated transmission lines required to transmit this power with one line out of service for the following cases: (a) 345-kV lines, $Z_c = 300 \Omega$, (b) 500-kV lines, $Z_c = 275 \Omega$, (c) 765-kV lines, $Z_c = 260 \Omega$. Assume that $V_S = 1.0$ per unit, $V_R = 0.95$ per unit, and $\delta_{\max} = 35^\circ$.
- 5.49 Repeat Problem 5.48 if it is desired to transmit: (a) 3200 MW to a load center located 300 km from the plant, (b) 2000 MW to a load center located 400 km from the plant.
- 5.50 A three-phase power of 3600 MW is to be transmitted through four identical 60-Hz overhead transmission lines over a distance of 300 km. Based on a preliminary design, the phase constant and surge impedance of the line are $\beta = 9.46 \times 10^{-4}$ rad/km and $Z_C = 343 \Omega$, respectively. Assuming $V_S = 1.0$ per unit, $V_R = 0.9$ per unit, and a power angle $\delta = 36.87^\circ$, determine a suitable nominal voltage level in kV, based on the practical line-loadability criteria.
- 5.51 The power flow at any point on a transmission line can be calculated in terms of the $ABCD$ parameters. By letting $A = |A|/\angle\alpha$, $B = |B|/\angle\beta$, $V_R = |V_R|/\angle 0^\circ$, and $V_S = |V_S|/\angle\delta$, the complex power at the receiving end can be shown to be
- $$P_R + jQ_R = \frac{|V_R| |V_S| / \beta - \alpha}{|B|} - \frac{|\delta| |V_R|^2 / \beta - \alpha}{|B|}$$
- (a) Draw a phasor diagram corresponding to the above equation. Let it be represented by a triangle $O'OA$ with O' as the origin and OA representing $P_R + jQ_R$.
- (b) By shifting the origin from O' to O , turn the result of (a) into a power diagram, redrawing the phasor diagram. For a given fixed value of $|V_R|$ and a set of values for $|V_S|$, draw the loci of point A , thereby showing the so-called receiving-end circles.
- (c) From the result of (b) for a given load with a lagging power factor angle θ_R , determine the amount of reactive power that must be supplied to the receiving end to maintain a constant receiving-end voltage, if the sending-end voltage magnitude decreases from $|V_{S1}|$ to $|V_{S2}|$.
- 5.52 (a) Consider complex power transmission via the three-phase long line for which the per-phase circuit is shown in Figure 5.20. See Problem 5.37 in which the short-line case was considered. Show that

$$\text{sending-end power} = S_{12} = \frac{Y'^*}{2} V_1^2 + \frac{V_1^2}{Z'^*} - \frac{V_1 V_2}{Z'^*} e^{j\theta_{12}}$$

$$\text{and received power} = -S_{21} = -\frac{Y'^*}{2} V_2^2 - \frac{V_2^2}{Z'^*} + \frac{V_1 V_2}{Z'^*} e^{-j\theta_{12}}$$

where $\theta_{12} = \theta_1 - \theta_2$.

(b) For a lossless line with equal voltage magnitudes at each end, show that

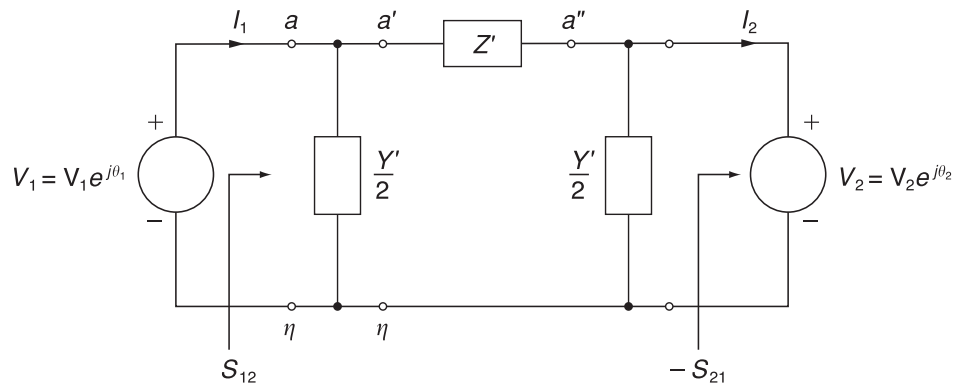
$$P_{12} = -P_{21} = \frac{V_1^2 \sin \theta_{12}}{Z_C \sin \beta \ell} = P_{\text{SIL}} \frac{\sin \theta_{12}}{\sin \beta \ell}$$

(c) For $\theta_{12} = 45^\circ$, and $\beta = 0.002$ rad/km, find (P_{12}/P_{SIL}) as a function of line length in km, and sketch it.

(d) If a thermal limit of $(P_{12}/P_{\text{SIL}}) = 2$ is set, which limit governs for short lines and long lines?

FIGURE 5.20

Per-phase circuit for Problem 5.52



PW

5.53 Open PowerWorld Simulator case Example 5_8. If we require the load bus voltage to be greater than or equal to 730 kV even with any line segment out of service, what is the maximum amount of real power that can be delivered to the load?

PW

5.54 Repeat Problem 5.53, but now assume any two line segments may be out of service.

SECTION 5.7

5.55 Recalculate the percent voltage regulation in Problem 5.15 when identical shunt reactors are installed at both ends of the line during light loads, providing 65% total shunt compensation. The reactors are removed at full load. Also calculate the impedance of each shunt reactor.

5.56 Rework Problem 5.17 when identical shunt reactors are installed at both ends of the line, providing 50% total shunt compensation. The reactors are removed at full load.

5.57 Identical series capacitors are installed at both ends of the line in Problem 5.14, providing 40% total series compensation. Determine the equivalent *ABCD* parameters of this compensated line. Also calculate the impedance of each series capacitor.

- 5.58** Identical series capacitors are installed at both ends of the line in Problem 5.16, providing 30% total series compensation. (a) Determine the equivalent $ABCD$ parameters for this compensated line. (b) Determine the theoretical maximum real power that this series-compensated line can deliver when $V_S = V_R = 1.0$ per unit. Compare your result with that of Problem 5.40.
- 5.59** Determine the theoretical maximum real power that the series-compensated line in Problem 5.57 can deliver when $V_S = V_R = 1.0$ per unit. Compare your result with that of Problem 5.38.
- 5.60** What is the minimum amount of series capacitive compensation N_C in percent of the positive-sequence line reactance needed to reduce the number of 765-kV lines in Example 5.8 from five to four. Assume two intermediate substations with one line section out of service. Also, neglect line losses and assume that the series compensation is sufficiently distributed along the line so as to effectively reduce the series reactance of the equivalent π circuit to $X'(1 - N_C/100)$.
- 5.61** Determine the equivalent $ABCD$ parameters for the line in Problem 5.14 if it has 70% shunt reactive (inductors) compensation and 40% series capacitive compensation. Half of this compensation is installed at each end of the line, as in Figure 5.14.
- 5.62** Consider the transmission line of Problem 5.18. (a) Find the $ABCD$ parameters of the line when uncompensated. (b) For a series capacitive compensation of 70% (35% at the sending end and 35% at the receiving end), determine the $ABCD$ parameters. Comment on the relative change in the magnitude of the B parameter with respect to the relative changes in the magnitudes of the A , C , and D parameters. Also comment on the maximum power that can be transmitted when series compensated.
- 5.63** Given the uncompensated line of Problem 5.18, let a three-phase shunt reactor (inductor) that compensates for 70% of the total shunt admittance of the line be connected at the receiving end of the line during no-load conditions. Determine the effect of voltage regulation with the reactor connected at no load. Assume that the reactor is removed under full-load conditions.
- 5.64** Let the three-phase lossless transmission line of Problem 5.31 supply a load of 1000 MVA at 0.8 power factor lagging and at 500 kV. (a) Determine the capacitance/phase and total three-phase Mvars supplied by a three-phase, Δ -connected shunt-capacitor bank at the receiving end to maintain the receiving-end voltage at 500 kV when the sending end of the line is energized at 500 kV. (b) If series capacitive compensation of 40% is installed at the midpoint of the line, without the shunt capacitor bank at the receiving end, compute the sending-end voltage and percent voltage regulation.
- PW** **5.65** Open PowerWorld Simulator case Example 5_10 with the series capacitive compensation at both ends of the line in service. Graph the load bus voltage as a function of load real power (assuming unity power factor at the load). What is the maximum amount of real power that can be transferred to the load at unity power factor if we require the load voltage always be greater than 0.85 per unit?
- PW** **5.66** Open PowerWorld Simulator case Example 5_10 with the series capacitive compensation at both ends of the line in service. With the reactive power load fixed at 500 Mvar, graph the load bus voltage as the MW load is varied between 0 and 2600 MW in 200 MW increments. Then repeat with both of the series compensation elements out of service.

CASE STUDY QUESTIONS

- A. For underground and underwater transmission, why are line losses for HVDC cables lower than those of ac cables with similar capacity?
- B. Where are back-to-back HVDC converters (back-to-back HVDC links) currently located in North America? What are the characteristics of those locations that prompted the installation of back-to-back HVDC links?
- C. Which HVDC technology can independently control both active (real) power flow and reactive power flow to and from the interconnected ac system?

REFERENCES

- 1. Electric Power Research Institute (EPRI), *EPRI AC Transmission Line Reference Book—200 kV and Above* (Palo Alto, CA: EPRI, www.epri.com, December 2005).
- 2. Westinghouse Electric Corporation, *Electrical Transmission and Distribution Reference Book*, 4th ed. (East Pittsburgh, PA, 1964).
- 3. R. D. Dunlop, R. Gutman, and P. P. Marchenko, “Analytical Development of Loadability Characteristics for EHV and UHV Lines,” *IEEE Trans. PAS*, Vol. PAS-98, No. 2 (March/April 1979): pp. 606–607.
- 4. W. D. Stevenson, Jr., *Elements of Power System Analysis*, 4th ed. (New York: McGraw-Hill, 1982).
- 5. W. H. Hayt, Jr., and J. E. Kemmerly, *Engineering Circuit Analysis*, 7th ed. (New York: McGraw-Hill, 2006).
- 6. M. P. Bahrman and B. K. Johnson, “The ABCs of HVDC Transmission Technologies,” *IEEE Power & Energy Magazine*, 5, 2 (March/April 2007): pp. 32–44.